Ministry of Higher Education and Scientific Research
University of Baghdad
Institute of Laser for Postgraduate Studies

The performance of Bow-tie optical nanoantenna

A Thesis Submitted To The Institute Of Laser For Postgraduate Studies, the University Of Baghdad In Partial Fulfillment Of The Requirements For The Degree Of Master Of Laser / Electronics And Communication Engineering

By
Ghufran A.Alkader Hassan
B.Sc. Laser and Opto Electronic
2008

Supervisor by
Lecturer -Dr. Jawad A. Hasan

2020 AD **1441 AH**

بسم الله الرحمن الرحيم

﴿ يَرْفَعِ اللَّهُ الَّذِينَ آمَنُوا مِنْكُمْ وَالَّذِينَ أُوتُوا
الْعِلْمَ دَرَجَاتٍ وَاللَّهُ بِمَا تَعْمَلُونَ خَبِيرٌ ﴾

سورة المجادلة   الاية:(11)

صدق الله العظيم

Dedication

To express my appreciation to those who Supported and encouraged me, I dedicate this thesis

To…………..

…………………. My Family

………………….. My Relatives

………………….. My Friends

Ghufran A. AL.kader

Acknowledgments

First and foremost, I am grateful to the creator "ALLAH" for giving me the strength, enablement, knowledge, and understanding required to complete this work.

I am heartily thankful to my supervisor, **Dr. Jawad A. Hasan**, whose encouragement, guidance, and support from the initial to the final level enabled me to develop and understand the project. I would like to thank Prof. Dr. **Hussain Ali Jawad**, the Dean of the Institute of Laser for Postgraduate Studies and for welcoming me into their groups, and for his continued help and encouragement through this work. Also, I would like to introduce a great thank to **Dr. Mohamed K. Dhahir** who helped me so many times. And to **Hassanein radif.**

I would like to thank to all the staff of the Institute for their effort during this research work.

Last but not least we would like to express our gratitude to our friends and respondents for the supports Special thanks also go to all the members of the Photonic Department for their help and encouragement.

Abstract

Nanoantennas have been used in many application in communication for wireless data transfer at very high rate, medicine, chemistry, terahertz detection, and nanophotonic applications.In this study, the aim of the research is to study the performance and the resonance frequency, s-parameter and the directivity of the (Bowtie nanoantenna) in different dimensions such as (the gap distance, Thickness, and angle,) of the Bowtie nanoantenn with different material such as (gold,nickel,silver,and aluminum).The performance of optical Bowtie nanoantenna was studied by using the computer simulation technology (CST)programe by using finit integration teqnique (FIT) to design two types of the Bowtie nanoantenna (the Bowtie nanoantenna with a tip and with a flat edge) . It is put on a dielectric substrate to get a plasmonic nanoantenna , and explain how the response of the Bowtie nanoantenna is affected by changing its dimensions and the materials used .

It was found that the optimum length for Bowtie nanpoantenna is (130 nm) ,the width is (140 nm), the thickness is (20 nm), and , the gap distance of Bowtie nanoantenna (5 nm) with the gold material. The S-parameter is (-33 dB) and the resonance frequency is (377.3 THz).

The near field is the highest at gap distance (30 nm) because of the resonance frequency is (310.23 THz) .and We conclude that removing the feeding of flat edge Bowtie nanoantenna with an (aluminum) material, leads to an increase in the (s-parameter to (-12.98 dB).

All parameters of bow tie optical nanoantenna are better than that of the flat-edge Bowtie nanoantenna

That Bowtie nanoantenna can be used in many applications such as in the field of communication(because it can work at multiple frequency), Medicine, and biology.

Table of Contents

List of Abbreviations

SP	Surface Plasmons
DTH	Direct to Home
ACOMDs	Antenna-coupled metal– oxide–metal diodes
IR	Infrared
5G	Five Generation
SPP	Surface Plasmon Polarization
CPW	Coplanar waveguide
LSPRs	localized surface plasmon resonances
SPP	Surface plasmon polaritons
VSWR	Voltage standing wave ratio
G	Gain
MOM	metal– oxide–metal
Cst	Computer simulation technology
SERS	Surface-enhanced Raman scattering
3D	Three Dimension
2D	Two Dimension
1D	One Dimension
FIT	Finite integration technique
E_t	Electric field

$E_\circ$	Incident electric field
ρ	Conductivity
J	Current density
∇	Dual parameter
μ	Permeability
ω_o	resonance frequency
HFSS	High frequency structure simulator
MWS	Microwave studio
Si	Silicon
THZ	Terahertz
dB	Decibel
Nm	Nanometer
ω_p	Plasmon frequency
Ev	Electron volt
Γ	Reflection coefficient
Au	Gold
S11	s-parameter
f_{fp}	Fabry-Perot resonance frequency
$c_\circ$	Speed of light in Vacuum

ε_{sub}	Permittivity of substrate
λ	Wavelength
V/M	Volt on meter
VSWR	Voltage standing wave ratio
La	Length of antenna
Wa	width of antenna
Ta	thickness of antenna
G	Gap distance
Ls	Length of substrate
Ws	width of substrate
Ts	thickness of substrate
α	Alpha
Lr	Length of reflector
Wr	width of reflector
Tr	thickness of reflector

List of Figures

List of Tables

CHAPTER ONE

Introduction and Basic Concepts

1.1 Introduction

In chapter introduces the basic concepts of plasmonic and optial nanoantenna , discussing its principal properties and most important applications. Background and literature survey, motivation and objectives of the research.over the past decades ,

The study of optical phenomena and its techniques in the nanometer (nm) scale is called a nano-optics [1]. Nanoantennas are used to convert electromagnetic wave radiation into electric current and vise versa, so nanoantennas and antennas at radio frequencies and microwave are the same [1]**.**The radio frequency(RF) antennas are a good technology able to transmitting electromagnetic wave that is localized within alarge sub-wavelength [2].But in the operation of the nanoantennas at a visible wavelength is different from (RF) antennas and should be corrected the design and analysis rules to the nanoantennas [1]**.** So, the antennas could be work in the visible range of the electromagnetic spectrum when the dimension of the antennas is decreased to a nanometer range (nm) [3]**.** And the frequency is at (hundreds of terahertz) high frequency to operate in visible light. When the incoming radiation affects a dynamic current distribution to happen on an antenna, it is said to be a receiver, and when an externally actuated dynamic current distribution on the antenna causes radiation it is said to be a transmitter. Most antennas are reciprocal, which means that they both receive or transmit [4].

Antennas are usually represented with specific performance parameters: radiation power density, radiation pattern, beamwidth, radiation intensity, directivity, bandwidth, gain, input impedance, and polarization [5].

Guglielmo Marconi was the first who use the term “antenna” in radio context in 1895. Now, it is common to relate to electromagnetic transmitters or receivers as an antenna. They have been developed at the begining of electromagnetism theory and the need for enhancing the bandwidth of communication link has fed this development. Though, the development for antennas using shorter and shorter wavelengths did not touch the optical regime. One of the reasons for designing and improving optical frequencies, is that the need for using optical fibers and optical antenna in telecommunication applications are increased [6].

Optical antennas and their radio wave and microwave counterparts are like, but there are crucial differences in their physical features and scaling behavior since, at optical frequencies, metals are not ideal conductors, but heavily correlated plasmas characterized as a free electron gas. So, the penetration of radiation into metals cannot be ignored [7,8].

In this study, we try to investigate the plasmonic nanoantenna with its parameters. We select a Bowtie shape of nanoantenna because it represents the best to perform our purpose. The optical nanoantenna parameters are studied and analysed considering their effects on the resonance frequency and the field enhancement.

1.2 Aim of the work

This work aimed to study the effects of Bowtie nanoantenna parameters such as (length, shape, gap distance and thickness) on the nanoantenna response (performance) to an electromagnetic field (**laser source**). These performances are resonance frequency, reflection coefficient(S-parameter), the field pattern, and the directivity of a nanoantenna, using different types of metals such as (gold, silver, nickel, iron, aluminum).The silicon is used as a dielectric substrate. This work is done using (CST) program by (FIT) methods .

1.3 Types of nanoantenna

Based on the structure of antennas, they classified into the following types:

1) Wire Antennas – Dipole, Loop:

Wire antennas are designed in various forms such as dipole which is one of the simplest forms of directional antennas. The dipole is also identified as 'Half Wave Dipole' as the physical length of the antenna is half of the wavelength of operation [9].

The frequency and wavelength of a signal are related as

$$\mathbf{f = C / \lambda} \ldots\ldots\ldots..(\mathbf{1.1})$$

Where 'C': velocity of the light in free space [3×10^8 meter /second] λ : wavelength, and 'f': frequency of the operation [9].

The half-wavelength of the dipole antenna has a 1/2 cycle of the common distribution. The greatest of the common distribution is at the vertical directions and the common distribution decreases to '0' at the antenna edges. Thus, the pattern of radiation of the dipole has the minima at the antenna axis ends and maxima at vertical directions [9].

2) Aperture Antennas – Horn Antenna.

The Aperture antenna is supplied with such a short gap. The Horn antenna is recognized as a perfect aperture antenna. Depending on the orientation of this antenna, it is identified as 'Pyramidal Horn' 'H-plane Horn' and 'E-Plane Horn'antenna. Horn antennas have greater directivity and narrower bandwidth. Horn antenna is utilized as the test antenna in the calculation of gain in the standard gain measurement method [9].

3) Reflector Antennas – Parabolic and Corner reflector antennas.

The antennas which can have higher gain by reflecting EM waves on a surface are identified as 'Reflector Antenna'. Depending on the form of surface, this antenna is classified as a parabolic reflector antenna. This antenna is utilized for satellite reception and has been utilized for satellite Television signal reception. 'Direct to Home [DTH] Service' is also using this antenna. At the focal point of this antenna, a feed antenna is located. Dipole or horn antenna is utilized as a feeder for this antenna [7]. To enhance the efficiency of this antenna, the feeder is placed at the backside of the reflector. This is identified as 'Cassegrain feed'. Similarly, the feeder placed at one end is identified as 'Offset feed'. This antenna acts as an excellent microwave reflector and concentrates signal in a particular direction. Therefore, This antenna shows better directivity [9].

4) Array Antennas – Yagi- Uda Antenna.

The most comfortable and efficient directional antenna is the 'Yagi – Uda' Antenna. It is called after its inventors Uda and Yagi. This antenna has been successfully utilized for the very high frequency (VHF) band terrestrial home Television reception[10]. The directivity is enhanced by improving the number of directors which are identified as 'Parasitic Elements' as they are not directly fed. Only the dipole or folded dipole is directly fed. There is one reflector which utilized to reflect EM signal [9].

5) Patch Antennas – Microstrip antenna.

The idea of 'Microwave Integrated circuits' was enhanced in the 1970s. But this field did not enhance in an emerging field until introducing concepts of VLSI(very large scale integration). After the late 1980s, this field has a lot of enhancements. “Planar antennas” are offered according to this idea. Lines of transmission were enhanced according to dielectric substrate materials. The length and width of the conducting line are styled based on the dielectric constant and the operating frequency of substrate materials. Microstrip antenna has fewer benefits like low easy to fabricate, profile, easy to apply easy to feed, as an array, and hemispherical radiation pattern with middle directivity from 6-8 dB. Also, microstrip antennas have some obstacles like low efficiency and low bandwidth [9].

6) Depends on the radiation pattern, antennas generally fall into two categories:

1) **Directional**
2) **Omnidirectional.**

Omnidirectional antennas radiate RF energy equally in all horizontal directions which covers 360 degrees. It is also named ‘Non-Directional’ as it does not prefer any direction [9].

1.4 Optical nanoantenna

An optical antenna is a (rectifying antenna) that works with visible or infrared light. An antenna is a circuit containing an antenna and a diode, which turns electromagnetic waves into direct current . While antennas have long been used for radio waves or microwaves, an optical antenna operates in the same way, but with infrared or visible light, turning it into electricity.

It is vastly more challenging in practice to make an optical antenna. The challenge is that antennas tend to be similar in size to a wavelength, so a very tiny optical antenna requires a challenging nanotechnology fabrication process. A 2nd challenge is that, being very small, an optical antenna typically absorbs very little power, and therefore tend to produce a tiny voltage in the diode, which leads to low diode nonlinearity and hence low efficiency. Due to these and other challenges, optical antennas have so far been restricted to laboratory demonstrations, typical with intense, focused laser light producing a tiny but measurable amount of power [2].

Nevertheless, it is hoped that arrays of optical antenna could eventually be an efficient means of converting sunlight into electric power, producing solar power more efficiently than conventional solar cells.

The theory behind optical antennas is essentially the same as for traditional (radio or microwave) antennas. Incident light on the antenna causes electrons in the antenna to move back and forth at the same frequency as the incoming light. This is caused by the oscillating electric field of the incoming electromagnetic wave. The movement of electrons is an alternating current (AC) in the antenna circuit. To convert this into direct current (DC), the AC must be rectified, which is typically done with a diode. The resulting DC current can then be used to supply an external load. The resonant frequency of antennas (the frequency which results in lower impedance and thus highest efficiency) scales linearly with the physical dimensions of the antenna according to simple microwave antenna theory [61].

1.5 Properties of nanoantenna

1.5.1 S-parameter

S-parameter is the parameter of the relation between terminals in the electrical system. It is called a (reflection coefficient). It describes the value of the power that returned from the antenna. It could be written as a gamma (Γ) called return loss [4].

When s-parameter (s11) is = -10dB this means if 3 dB of power is transferred to the antenna -7db of the power will be reflected. The base of the power was allowed to the antenna, this allowed power may be emitted or absorbed as a hurt in the antenna [10].

If (s11) is 0db this meaning no power is radiated all power will be reflected from the antenna [10]

The matrix form of S-parameter as shown in the equations of (1.2 and 1.3):

$$\begin{bmatrix} \boldsymbol{b1} \\ \boldsymbol{b2} \end{bmatrix} = \begin{bmatrix} \boldsymbol{S11} & \boldsymbol{S12} \\ \boldsymbol{S21} & \boldsymbol{s22} \end{bmatrix} \begin{bmatrix} \boldsymbol{a1} \\ \boldsymbol{a2} \end{bmatrix} \dots\dots\dots..(\mathbf{1.2})$$

$$\mathrm{S}= \begin{bmatrix} \boldsymbol{S11} & \boldsymbol{S12} \\ \boldsymbol{S21} & \boldsymbol{S22} \end{bmatrix} \dots\dots\dots..(\mathbf{1.3})$$

The above equation is called a scattering matrix.

S11 is the input port voltage reflection coefficient.

S12 is the reverse voltage gain.

S21 is the forward voltage gain.

S22 is the output port voltage reflection coefficient.

A is the wave traveling towered the-port 1.

B is the wave going away from the-port 2.

1.5.2 Radiation Patterns

In the antenna design field, the term, pattern of radiation (or far-field pattern or antenna pattern) indicates the angle (directional) dependence of the radio wave's strength from the antenna or other sources. In other words, The radiation pattern describes the directional variation of achievement parameters in the transmitter antenna. The trace of the magnetic or electric field at the constant distances from the antenna is the amplitude field pattern while an alike trace of magnetic or electric power density is the amplitude power pattern. However, the radiation pattern normally has bulging portions named lobes [11]. Lobes of radiation are high-intensity directions surrounded by weaker radiation directions. The main lobe includes the maximum radiation direction which was the desired radiation direction. Any lobe other than the major lobe is a minor lobe. The radiation pattern of the antenna alters according to distance from the antennas. These changes in the field pattern in the space surrounding antennas are separated into 3 field areas: Fresnel (radiating near field), Fraunhofer (far-field), and reactive near field. However, the reactive near field areas start from radiating surfaces of antennas and terminate the wavelength of transceiver waves [12]. In the current area, the energies decay very quickly with the distance from radiating surfaces (energies decay with the 3rd and 4th power of the distances) and the field patterns are approx. Homogeneous. However, the Fresnel (radiating near field) pattern was most usually identified over the spherical or cylindrical surfaces or the placed plane in front of sources, enclosing it [60]. The antenna far-field pattern may be limited in the range of the antenna, or an alternate, the near-field pattern maybe exist by the near-field scanner.The far-field radiation pattern can be determined from the shape of the antenna using computer programs like NEC(Nipon Electronics Company) software. Other software, such as HFSS (High-frequency structure simulator), can also determine the near field. The far-field radiation pattern may be imaged graphically as a plot of one of several associated variables, involving; the strength of the field at the constant (large) radius (the pattern field or amplitude pattern), the directive gain, and the power per unit solid angle (power pattern). Very often, just the relative amplitude is plotted, normalized either to the total radiated power or to the amplitude on the antenna boresight. The plotted quantity may be exhibited in dB or on the linear scale. Typically, the plot is imaged as three-dimensional graphs (at right), or as separate graphs in the horizontal and vertical plane. Often, this is called the polar diagram [13].

1.5.3 Voltage standing wave ratio (VSWR)

The VSWR (Voltage Standing Wave Ratio) was the sign of mismatch amount between the antenna and the feeding line attaching to it. The scale of values for VSWR is from 1 to ∞. A VSWR value under 2 is estimated properly for most antenna applications. The antenna can be described as having a good match. So when someone says that the antenna is badly matched, it means that the VSWR value exceeds 2 for a frequency of interest [13].

1.5.4 Gain

In electro-magnetics, the power gain of antenna or simply gain (G) is a key complete number that binds the directivity and efficiency of antenna. In the transmitting antennas, the gain shows how well the antenna transfers input power in waves of radio headed in the special direction. In the receiving antennas, the gain shows how well antennas convert the arrived radio waves from the special direction to the power of electricity. When no direction is specified, "gain" is understood to refer to the value of the peak of the gain, the gain in the direction of the antenna's main lobe. A plot of the gain as a function of direction is known as the radiation pattern or gain pattern [12].

The gain G of the antenna was the ratio of the intensity U of radiation in the special direction to the intensity of antenna input power averaged over all directions.

Again, if the special direction isn’t defined, it is utilized to be the direction of the greatest radiation. A constantly called efficiency of radiation ecd is named in order to relate input and intensities of radiated power

$$\boldsymbol{p_{rad} = ecd * P_{in}}\text{……}\mathbf{(1.4)}$$

Where is P rad is the power radiation

and ecd is radiation efficiency [12].

1.5.5 Directivity

In electromagnetism, directivity is the parameter of the optical system or antenna that determines the degree of concentration of radiation emitted in a single direction. It also determines the radiated power density using the antenna in the direction of its strongest emission, versus the density of power radiated using the ideal isotonic radiator (which is uniformly emitted in all directions) radiating the same total power [12].

The directivity of the antenna is its gain element; the second thing is its efficiency (electrical). Directivity is a significant measure because different optical systems and antennas are designed to give radiation in the form of electro-magnetic waves at a narrow-angle or in one direction. Directivity is sometimes called an antenna that receives electro-magnetic waves, and its direction at reception is equal to that at the transmission.

The directivity D of the antenna is the ratio of the intensity of the radiation U in the particular direction to the intensity of radiation averaged over all directions U0 = Prad/4π. If the specific direction isn't allocated [12].

$$\boldsymbol{D = \frac{U}{U_0} = \frac{U}{P_{rad}/4\pi}} \ldots\ldots\ldots..(\mathbf{1.5})$$

Where **U0** is the radiation intensity and **Prad** is the power radiation.

1.5.6 Efficiency

Radiation efficiency embodies conduction and dielectric losses of the antenna. It does not involve the mismatch loss between the source and guiding device couple and the antenna. Thus directivity and gain are related [13].

$$\boldsymbol{G = \frac{U}{Pin/_{4\pi}} = e_{cd}D} \ldots\ldots\ldots..(\mathbf{1.6})$$

Where is the Pin is the amount of power coupled to the antenna, G is the gain, ecd radiation efficiency and U is the radiation intensity.

1.5.7 Bandwidth

The antenna bandwidth is the frequencies range where parameters of the antenna achievement have the agreeable value comparison with these at a center frequency of the antenna [12].

1.5.8 Polarization

The antenna polarization is the electro-magnetic polarization of the wave radiated in a specific direction. If the specific direction isn't defined, it is taken to be the direction of greatest gain. However, polarization was classified as circular, elliptical, and linear. If the magnetic or electric field vectors of radiated waves at a point is usually directed along the line at every time instant, the field is assumed to be linearly polarized [12,14].

1.6 Bowtie nanoantenna

In the communication network system, the dense, effective, and low-cost devices have been extremely needed. In the manufacturing of advanced antenna, A bow-tie antenna is also known as the Biconical antenna or Butterfly antenna. Biconical antenna is an omnidirectional wide-band antenna. According to the size of this antenna, it has low- frequency response and acts as a high-pass filter. As the frequency goes to higher limits, away from the design frequency, the radiation pattern of the antenna gets distorted and spreads. Most of the bow-tie antennas are derivatives of biconical antennas. As shown in Figure (1-1) The discount is a type of half-biconical antenna. The bow-tie antenna is planar, and therefore it is considered as directional antenna[15].

The output limitation is based on place, distance, and alignment of the suggested antenna. Effective applications of these antennas are mobile communication networks and wireless systems [16]. The shape of a Bowtie antenna is seen in Figure(1-1)[16].

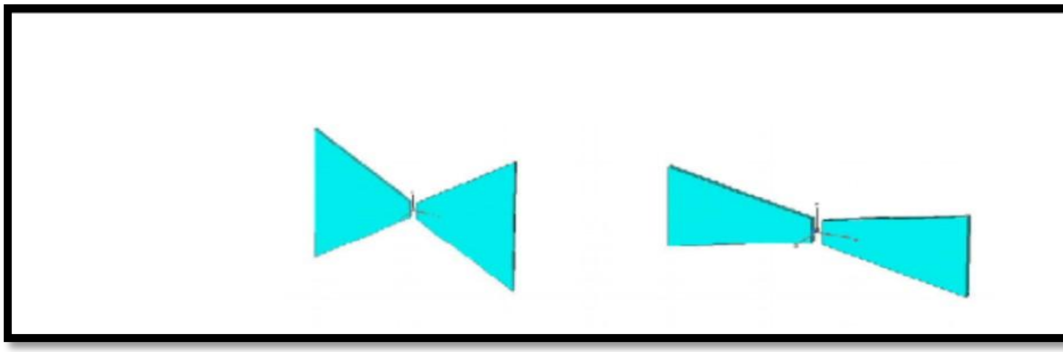

Figure (1.1) Bowtie antenna[16]

Instead of being constructed with a conductor sheet, the Bowtie antenna can be constructed using a wire to form the same shape. This is beneficial because it is lower cost because of less is being used metal and decreases wind resistance. The bow-tie antenna is center-fed like a dipole. Figure (1-2) illustration of a wire Bowtie antenna.[16].

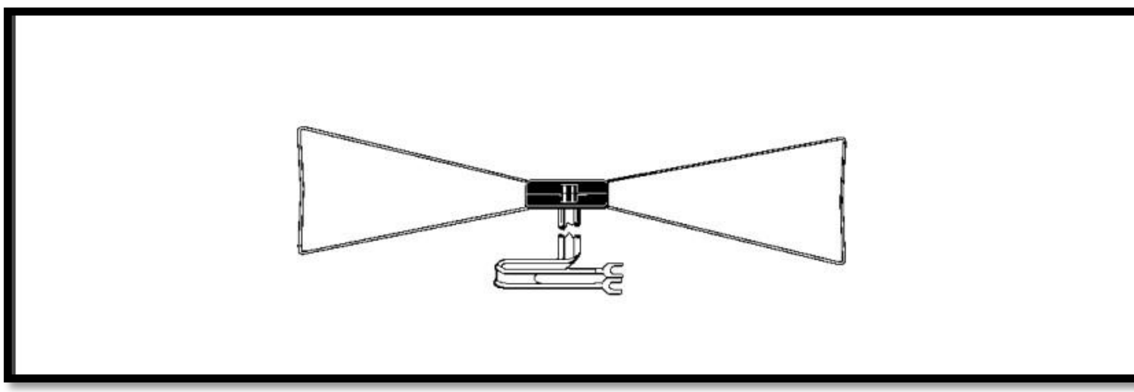

Figure (1.2) Wire Bowtie Antenna [16]

As you can see in Figure (1-2) the metal used to construct this dipole is significantly less than a traditional Bowtie antenna constructed from sheet metal. This method will lower production costs and decrease the weight of the antenna.

1.7 Application of nanoantenna

There are many applications of nanoantenna in the medicine (diagnosis, drug delivery, textile engineering) [17], in the chemistry and environmental (stimulus), in the information and communications (semiconductor devices, optical devices) [5].and nanoantenna for terahertz detection, wireless data transfer at very high rate, and nanophotonic applications [18].

1.7.1 Optical Wireless Link:

The nanoantennas have a great ability to control the direction and angle of the optical beam on the broad spectrum. The nanoantennas are one of the main elements that go into the field of optical communication because of its involvement in the manufacture of nanocircuits. The transmission of optical waves power will be in the near future by plasmonic nanoantennas in the far-field of transmission and the receiving process of the beam signals will be by the nanoscopic receivers [18, 19].

1.7.2Nanoantenna for Terahertz Detection

Infrared detectors are essential devices in, e.g., security and medical fields. Antenna-coupled metal– oxide–metal diodes (ACMOMDs) are a promising candidate for infrared (IR) detectors due to their little size, CMOS compatibility, and ability to offer full functionality without cooling or implemented bias. The idea of ACMOMD was first started in the 1970s. The device consists of two main elements: the dipole antenna for receiving electromagnetic waves in a certain wavelength range and a metal– oxide–metal (MOM) diode that serves as the rectifying device [20,21].

1.7.3 Nanoantenna for Nanophotonic Application

Antennas work an essential role in many microwave applications [22]. But, recent developments of antennas in the near-infrared and optical areas are giving great promises with better manipulation, emission control, and radiation of light waves into free space. In current years, nanoscale optical antennas are recommended for many applications in the near-infrared, far-infrared, and visible range. For example, nano-antennas have been recognized as an efficient and promising component in scattering, sensing, photo-detection, heat-transfer, inter and/or intra chip optical communications, energy harvesting, etc. Furthermore, optical nanoantenna can work a vital role in decreasing power consumption and allow higher speed for on-chip optical interconnects [23,24].

1.7.4 Mobile Communication

The 5G mobile connection in the next decade is moving to require 1000 times' larger bandwidth and 100 times more speed to cover a large number of applications of future cell phones. One of the expected techniques to fulfill these elements is moving to be a THz band mobile connection. This would certainly want the THz band nanoantennas [25].

1.8 The boundary condition of nanoantenna

In many physical situations, the medium is piecewise homogeneous. In this case, the entire space is divided into subdomains in which the material parameters are independent of position. In principle, a piecewise homogeneous medium is inhomogeneous However, the inhomogeneities are entirely confined to the boundaries and it is convenient to formulate the solution for each subdomain separately. These solutions must be connected with each other via the interfaces to form the solution for all space. Let the interface between two homogeneous domains Di and Dj be denoted as ∂Dij. If εi and μi designate the constant material parameters in subdomain Di, the wave equations in that domain read as [26].

$$(\boldsymbol{\nabla}^2 + \boldsymbol{k}^2\, \boldsymbol{i})\boldsymbol{Ei} = -\, \boldsymbol{i\omega}\mu 0\mu \boldsymbol{i}\, \boldsymbol{ji} + \boldsymbol{\nabla\rho i} / \boldsymbol{\varepsilon 0\varepsilon i} \text{ .... (1.7)}$$

$$(\boldsymbol{\nabla}^2 + \boldsymbol{k}^2\, \boldsymbol{i})\boldsymbol{Hi} = -\boldsymbol{\nabla} \times \boldsymbol{ji} \text{ ...... (1.8)}$$

$$\text{where } \boldsymbol{ki} = \left(\frac{\boldsymbol{\omega}}{\boldsymbol{c}}\right)\sqrt{\ }\boldsymbol{\mu}\mathbf{i}\ \boldsymbol{\varepsilon}\mathbf{i} \text{.......(1.9)}$$

$\boldsymbol{ki}$ is the wavenumber and ji, ρi the sources in domain Di. To obtain these equations, the identity $\boldsymbol{\nabla} \times \boldsymbol{\nabla} = -\boldsymbol{\nabla}^{\,2} + \boldsymbol{\nabla\nabla}$ was used in Maxwell's equations.

Equations(1.7)and(1.8)are also denoted as the inhomogeneous vector Helmholtz equations. In most practical applications, such as scattering problems, there is no source current so recharges present and the Helmholtz equations are homogeneous.

Since the material properties are discontinuous on the boundaries, Eqs. (1.7) and (1.8) are only valid in the interior of the subdomains. However, Maxwell's equations must also hold for the boundaries. Due to the discontinuity, it turns out to be difficult to apply the differential forms of Maxwell's equations, but there is no problem with the corresponding integral forms. The latter can be derived by applying the theorems of Gauss and Stokes to the differential forms (1.10)–(1.11) which yields [26,1].

$$\boldsymbol{\nabla} \times \boldsymbol{E}(\boldsymbol{r},\boldsymbol{t}) = -\,\frac{\partial \boldsymbol{B}(\boldsymbol{r},\boldsymbol{t})}{\partial \boldsymbol{t}} \text{ ......(1.10)}$$

$$\boldsymbol{\nabla} \cdot \boldsymbol{B}(\boldsymbol{r},\boldsymbol{t}) = \mathbf{0} \text{ .... (1.11)}$$

$$\int \mathbf{E}(\mathbf{r},\mathbf{t}) \cdot \mathbf{ds} = -\int \frac{\partial}{\partial \boldsymbol{t}} \boldsymbol{B}(\boldsymbol{r},\boldsymbol{t}) \cdot \boldsymbol{ns}\ \boldsymbol{da} \text{.......(1.12)}$$

$$\int \mathbf{H}(\mathbf{r},\mathbf{t}) \cdot \mathbf{ds} = \int [\mathbf{j}(\mathbf{r},\mathbf{t}) + \frac{\partial}{\partial \boldsymbol{t}} \mathbf{D}(\mathbf{r},\mathbf{t})] \cdot \mathbf{ns\ da} \text{ ..... } (\mathbf{1.13})$$

$$\int \boldsymbol{D}(\boldsymbol{r},\boldsymbol{t}) \cdot \boldsymbol{ns}\ \boldsymbol{da} = \int \boldsymbol{\rho}(\boldsymbol{r},\boldsymbol{t})\ \boldsymbol{dv} \text{ ....(1.14)}$$

$$\int \boldsymbol{B}(\boldsymbol{r},\boldsymbol{t}) \cdot \boldsymbol{ns}\ \boldsymbol{da} = \mathbf{0} \text{ ....(1.15)}$$

In these equations, da denotes a surface element, ns the normal unit vector to the surface, dV the surface of volume V, and dS the border of the surface S. The integral forms of Maxwell's equations lead to the desired boundary conditions if they are applied to asufficiently small part of the considered boundary. In this case, the boundary looks flat and the fields are homogeneous on both sides [26,27].

1.9 Plasmonic nanoantenna

The plasmonic nanoparticle is defined as particles with electron density sufficient to couple with the electromagnetic radiation of incident wavelengths. These nanoparticles are considerably large because of the nature of the dielectric-metal mediator between the medium and particles. Different in a pure metal where there is an utmost limit on what size wavelength can be effectively coupled rooted in the material size [28].

These particles are distinguished from standard surface plasmons in that plasmonic nanoparticles exhibit attractive absorbance, scattering, and coupling properties depending on their geometries and comparative positions [29]. These singular properties have made these particles a focus of research in several applications, including spectroscopy, communication, cancer treatment, solar cells and indicator of enhancement for imaging [30]. They are also good candidates for designing mecha-optical instrumentation given their high sensitivity [31].

Plasmons are oscillations of free electrons as a result of the formation of a dipole in the material caused by electromagnetic waves. The electrons move into the material to return to its initial state; however, the light waves oscillate, leading to the constant shift in the dipole, which results in the oscillation of the electrons at a frequency similar to that in light. This coupling occurs only when the frequency of the light is the same as or less than the plasma frequency and is utmost at the plasma frequency that is so-called the resonant frequency. Scattering cross-section and absorbance explain the density of a particular frequency to be scattered or absorbed. Several fabrication processes or chemical synthesis methods that rely on controllable size and geometry exist for the preparation of such nanoparticles [32].

The equations that characterize the absorbance and scattering cross-sections for very small nanoparticles are

$$\boldsymbol{\sigma_{scatt=\frac{8\pi}{3}} k^4 R^6 \left|\frac{\varepsilon_{particle} - \varepsilon_{medium}}{\varepsilon_{particle} + 2\varepsilon_{medium}}\right|^2 \cdots (1.16)}$$

$$\boldsymbol{\sigma_{scatt=\frac{8\pi}{3}} k^4 R^6 Im \left|\frac{\varepsilon_{particle} - \varepsilon_{medium}}{\varepsilon_{particle} + 2\varepsilon_{medium}}\right|^2 \cdots (1.17)}$$

where (κ) is the wavenumber, R is the radius of the particle,($\varepsilon_{particle}$) is the relative permittivity of the particle described by equation (1.18) [32].

, and ε_{medium} Is a relative permittivity of a dielectric substrate,

$$\boldsymbol{\varepsilon_{particle=1-\frac{\omega_p^2}{\omega^2+i\omega\gamma}} \cdots (3) \ldots\ldots (1.18)}$$

As we know as the Drude model for free electrons where ω_p^2 is the plasma frequency,γ is the relaxation frequency of the charge carriers and ω is a frequency of electromagnetic radiation. This equation is the consequence of solving the differential equation for a harmonic oscillator with a driving force proportionate to the electric field to the particle is exposed to.

It logically followed that the resonance case for these equations is reached as the denominator is at zero.

$$\boldsymbol{\varepsilon_{particle} + 2\varepsilon_{medium} \approx 0}$$

As this state is satisfied, the cross-sections are at their highest, These cross-sections are for single, spherical particles. The equations change when particles are nonspherical or are coupled to one or more other nanoparticles, for example when their geometry changes. This principle is important for several applications, Rigorous electrodynamics investigation of plasma oscillations in a spherical metal nanoparticle of a finite size is performed in [32].

1.10 Surface Plasmon polaritons (SPPs)

The energy received by metals such as gold and silver from the incident electromagnetic field isn’t lost. The energy has to proceed somewhere and because of the coupling between the electro-magnetic field and electrons (charged free particles in metals), the energy moves the electron, creating it's for oscillation in unison with the used electric field. The mass oscillation of electrons, called plasmons, is the oscillation of the plasma or electron gas that surrounds sites of the atomic lattice of metals. When a photon merges with plasmons, the produced semi-particle (called polariton) is distributed along the metal surfaces until decaying, except by being absorbed, in which case the energy is converted to the photon, or through a radiative transition to photons [33].

When plasmons are started at an interface of metal, they are identified as surface plasmons. The frequency of plasmon excitation is so dependent on the metal features and the geometry under consideration. That is, bulk metal plasmon excitation happens at a different incident frequency than for a film of metal interfacing a dielectric. If the metal is spherical or some other shape embedded in a dielectric, the frequency of plasmon oscillation will again be modified. [33].

SPPs (Surface plasmon polariton) are electro-magnetic waves transmitted with metal-air or metal-dielectric interface side by side, especially at visible or infrared frequencies. However, the term "surface Plasmon polariton " clarifies that the waves involve electro-magnetic waves in the dielectric or air ("polariton"), and the charging movement in the metal ("surface plasmon") [34].

They are a type of surface wave, guided along with the interface in the same way that light can be guided by an optical fiber. SPPs are shorter in wavelength than the incident light (photons). Hence, SPPs can have tighter spatial confinement and higher local field intensity. Perpendicular to the interface, they have subwavelength-scale confinement. An SPP will propagate along with the interface until its energy is lost either to absorption in the metal or scattering into other directions (such as into free space) [35].

Application of SPPs enables subwavelength optics in microscopy and lithography beyond the diffraction limit. It also enables the first steady-state micro-mechanical measurement of a fundamental property of light itself: the momentum of a photon in a dielectric medium. Other applications are photonic data storage, light generation, and bio-photonics. Control and manipulation of light utilizing SPPs on the nanometer scale display significant benefits in nanophotonics devices with so little elements and SPPs open a promising way in areas involving the environment, energy, biology, and medicine [35].

1.11 **Surface plasmon Resonance**

Surface plasmon resonance (SPR) is the resonant oscillation of conduction electrons at the interface between negative and positive permittivity material stimulated by incident light. SPR is the basis of many standard tools for measuring the absorption of material onto planar metal (typically gold or silver) surfaces or onto the surface of metal nanoparticles. It is the fundamental principle behind many color-based biosensor applications, different lab-on-a-chip sensors, and diatom photosynthesis. For the development almost a decade ago of the first biosensor based on surface plasmon resonance (SPR), the usefulness of this technique has developed steadily. Although there are several SPR based systems, by far the most widely utilized one is the Biacore (a life science products company), it is specialized in measuring a biomolecular interaction, which has grown into a range of instruments [36].

1.12 **Local surface Plasmon Resonance**

Localized surface plasmon resonance (LSPR) is the result of the confinement of the surface plasmon in the nanoparticles of a size comparable to or smaller than the wavelength of light used to excite the plasmon. The LSP has two important effects: electric fields near the particle’s surface are greatly enhanced and the particle optical absorption has a maximum at the plasmon resonant frequency. The enhancement falls off quickly with distance from the surface and, for noble metal nanoparticles, the resonance occurs at visible wavelengths. For semiconductor nanoparticles, the maximum optical absorption is often in the near-infrared and mid-infrared region. LSPR has emerged as a leader among label-free biosensing techniques in that it gives sensitive, robust, and facile detection. Traditional LSPR-based biosensing uses the sensitivity of the plasmon frequency to variations in the local index of refraction at the nanoparticle surface. Although surface plasmon resonance technologies are now widely applied to estimate bimolecular interactions, many challenges remain. they have characterized these challenges into four categories: improving sensitivity and limit of detection, selectivity in complex biological solutions, sensitive detection of membrane-associated species, and the adaptation of sensing elements for point-of-care diagnostic devices [37].

The interaction of the noble metallic nanoparticle with light presents a collective oscillation of conduction band electrons identified as the LSPR. Only the material with a negative real and little positive imaginary dielectric constant is capable to support the surface plasmon. The most common materials used are gold and silver, although other metals such as copper and aluminum also display plasmon resonance. When the incident electromagnetic field matches that of the oscillating electrons on the surface of the nanoparticle as shown in Figure (1-3) [37].

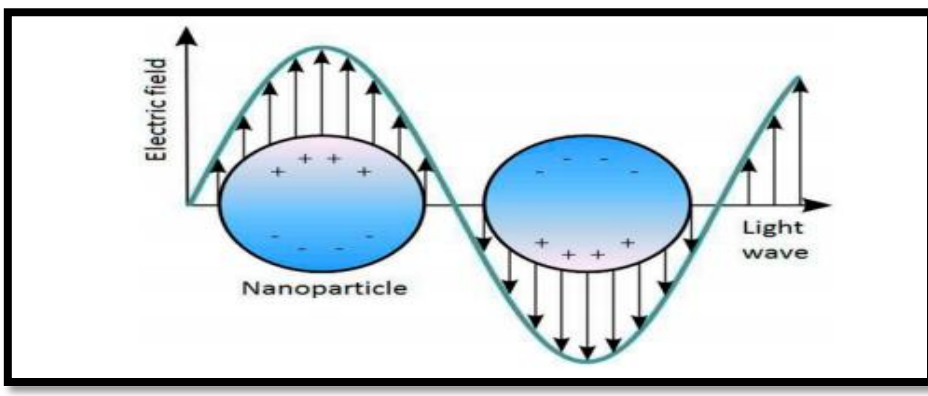

Figure 1.3: Schematic diagram illustrating the localized surface plasmon on a nanoparticle surface [37]

1.13 Drude –model

The optical response of noble metals in the frequency domain is described by a dispersive complex dielectric function, ε(ω). From a qualitative point of view the mechanisms that contribute to ε(ω) can be identified:

Response of conduction electrons: the concept of single electrons moving against a background lattice of positive ion cores can describe many of the fundamental electronic properties of the solid-state. Ignoring the lattice potential and electron-electron interactions, it ends up with a gas of free electrons in the metal that can be treated as an electron liquid of high density or plasma. Drude adopted this classical approach to describe the electron dynamics in a metal [38], and came up with the motion equation of a damped oscillator, where the electrons, subjected to an incident electric field, move between heavier relatively immobile ions:

Consider a typical electron denoted by $x = x(t)$ the deviation from its equilibrium position

External electric field strength $E = E(t)$

$$m\ddot{x} + b\dot{x} + kx = eE \quad \text{.......(1.19)}$$

Where m,e are mass and charge of an electron, b is damping factor

k is spring constant = 0 for metals

This is known as Drude-Sommerfeld model (or simply Drude model) of the free electron gas, where x is the displacement of the electron with respect to its rest position (˙ x and ¨ x represent the first and second-time derivatives, respectively), m is its effective optical mass (incorporating some aspects of the band structure), e its charge [38], And by solving this equation the dielectric function is

$$\varepsilon(\omega) = \varepsilon_1 + 2\varepsilon_2 \ldots\ldots (1.20)$$

$$\varepsilon_1 = \frac{\omega_p^2}{\omega_p^2 + \gamma^2} \ldots\ldots\ldots\ldots (1.21)$$

$$\varepsilon_2 = \omega_p^2 \frac{\gamma}{\omega^{\,2} + \gamma\omega} \ldots\ldots\ldots (1.22)$$

Where $$\omega_p^2 = \frac{ne^2}{m\varepsilon_\circ} \ldots\ldots\ldots (1.23)$$

$$\gamma = \frac{b}{m} \ldots\ldots\ldots (1.24)$$

Is the volume plasma frequency, with values lying in the ultraviolet region for most metals, $\varepsilon_\circ$ Being the permittivity of a vacuum. And $\gamma = 1/\tau$ is a motion damping factor accounting for collisions, being τ the relaxation time of the free electron gas [39].

1.14 Maxwell equation in Metamaterial and electromagnetic in metal

Metals can be considered as an isotropic medium with a dielectric function, ε, permeability μ, and conductivity σ. It is possible to write the Maxwell equations in metals by using the relationships between the electric field and these material quantities, D(r)=ε(r)E(r), B = μH, and J = σE where D is the electric displacement, J is the current density and B is the magnetic induction vector [40].

$$\nabla \cdot H = 0 \ldots\ldots\ldots\ldots (1.25)$$

$$\nabla . \bar{E} = \frac{\rho}{\varepsilon} \ldots\ldots\ldots\ldots (1.26)$$

$$\nabla \times \overline{\mathbf{E}} + \mu \frac{\partial \overline{\mathbf{H}}}{\partial \mathbf{t}} \ldots\ldots\ldots..(\mathbf{1.27})$$

$$\nabla \times \overline{\mathbf{H}} + \varepsilon \frac{\partial \mathbf{E}}{\partial \mathbf{t}} = \sigma \mathbf{E} \ldots\ldots\ldots..(\mathbf{1.28})$$

Where H magnetic field

E = eclectic field

ρ = charge density

From these equations, we can extract information on the material optical properties. (1.26) and (1.27) can be manipulated to eliminate H. If we consider monochromatic light and propose a plane wave solution to Maxwell's equations,

$$\boldsymbol{E} = \boldsymbol{E}_{\circ} \boldsymbol{e}^{-\boldsymbol{ikx}-\boldsymbol{i\omega t}} \ldots\ldots(1.29)$$

Then, the wave equations for metal can be written [41]:

$$\nabla^{2} + \omega^{2}\mu\left(\varepsilon + i\frac{\sigma}{\omega}\right)E = 0\ldots\ldots(\mathbf{1.30})$$

1.15 Literature review

A brief description of researches related to this approach is shown in the following paragraphs:

In 2008, Kumar, Anil; [42] presented a Bowtie with 240 nm height and ~10 nm gap as displayed in Figure. (1-4). Bright field illumination on this Bowtie array with a gold thickness of 50 nm and spacing of 3 µm provides an extinction peak at 960 nm as in Figure (1-5). Based on these measurements, utilizing a setup shown in Figure. (1-5) (inset), the extinction efficiency for this structure can be simply calculated i.e the extinction efficiency of a particle is provided by Qext = Cext / Cgeo where the geometrical cross-section, Cgeo = 0.0672 μm21 from these bright field measurements, recognized a peak Qext ~11 which is more than twice the value previously reported.

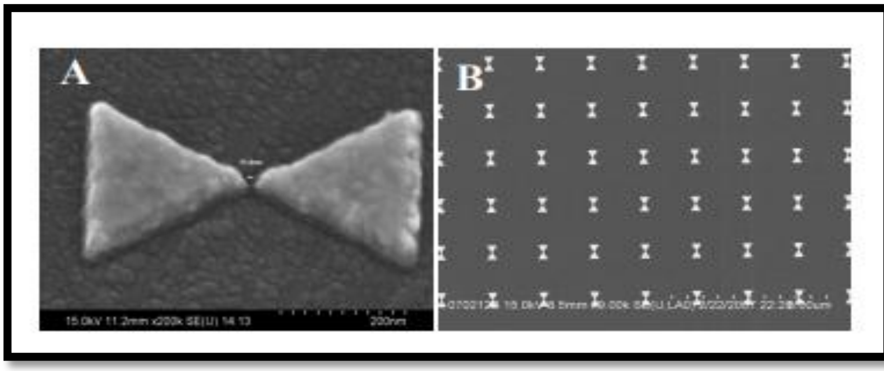

Fig.(1-4) SEM images of Bowtie antenna fabricated on glass/ITO substrate using electron beam lithography. The structure in (A) has a tip-to-base height of 240 nm and a gap ~ 10 nm; (B) shows an array of these Bowties with a spacing of 3 μm[42].

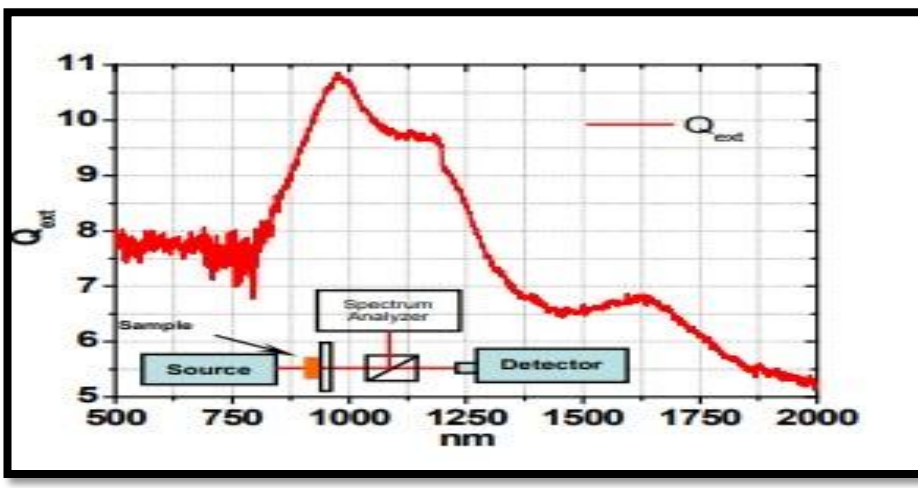

Figure 1.5: Extinction efficiency calculated from bright field illumination of a Bowtie antenna array. Schematic of the measurement setup is shown in the inset. A peak extinction efficiency of ~11, twice the value previously reported [42]

In 2010, Wen-Yu Chen1 and Chun-Hung Lin; [43]: The bow-tie antennas studied here are composed of two equilateral triangles with 200 nm sides. The gaps range from 20 nm to 60 nm; the thickness of the entire structure is 50 nm; the material of antennas is gold; the structures are free of the substrate. Based on electrostatic approximation (ESA), eigenvalue problems are solved to find out the resonant modes of bow-tie antennas. Figure (1-6) shows the surface charge distribution of fundamental mode of 40 nm gap bow-tie antenna. The charge is more concentrated on the gap. In other words, the electric field in the gap is enhanced by the coupling of triangles they proposed the way to find out the excitation amplitude at a resonating frequency based on the energy conservation theory. The near field plots of electric fields in parallel component with 40 and 60 nm gaps. The simulation is shown in Figure (1-7) There is a maximum in the middle of the 40 nm gap,

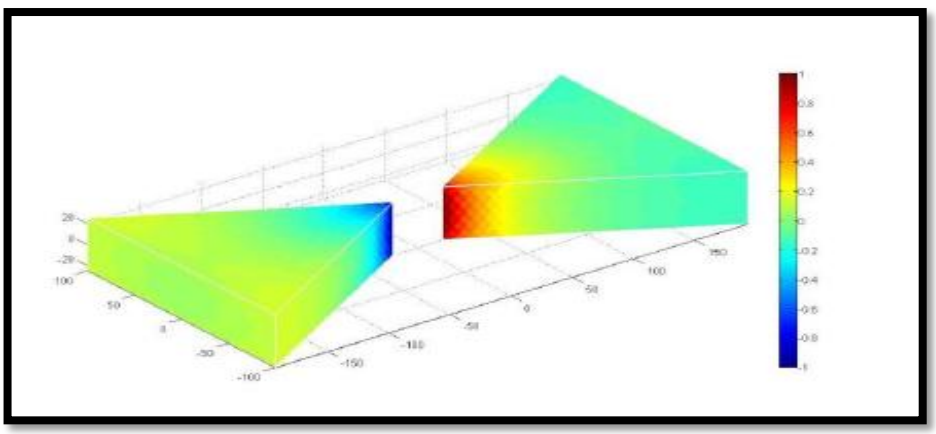

Figure 1.6: Charge distribution of the fundamental mode of bow-tie antenna with 40 nm gap [43]

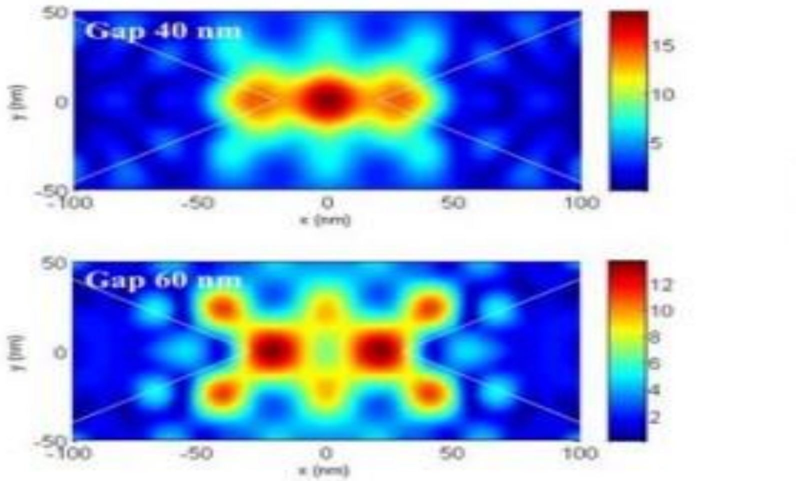

Figure 1.7 Near field plots of the parallel component with 40 and 60 nm gaps from RCWA simulation[43]

In 2010, Yu-Ming, et.al; [44] Assumed that the field patterns in the E -plane and -a plane is plotted in Figure (1-8). for the bow-tie shaped hole nanoantenna with a radius 30 nm of curvature and a flare angle of 60 at a wavelength of 500 nm. The patterns of the nanoantenna imply that a great directivity is available by the bow-tie hole. From Figure (1-8), it is seen that the half-power bandwidths achieved are 51.8v/m and 40.2 in both planes.

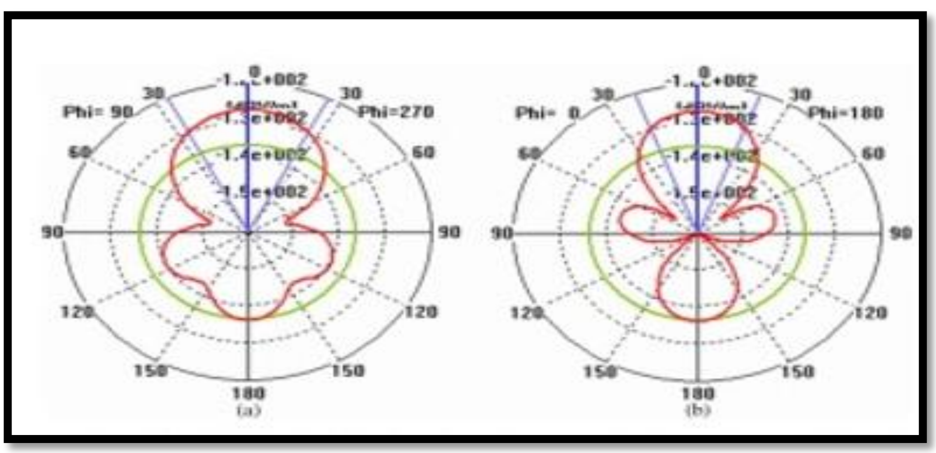

Figure 1.8: Field pattern of bow-tie shaped aperture nanoantennas -a- E-plane -b- H-plane [44]

In 2010, Thamae, Leboli Z, et.al, [45] Optimized A dielectric resonator antenna (DRA) notch and feed dimensions with a preferred height of 12.7 mm are found to be d=6.7mm, p=7mm and A Bowtie DRA prototype shown in Figure. (1-9 a) has been fabricated and experimented to validate the simulation results. The simulation and measurement reflection coefficient curves are depicted in Figure. (1-9 b) with respective impedance bandwidths of 53.7% (4.166–7.226 GHz) and 49.4% (4.194–6.944 GHz). The measured bandwidth is about 4% less than the simulated one but both responses present consistent variations.

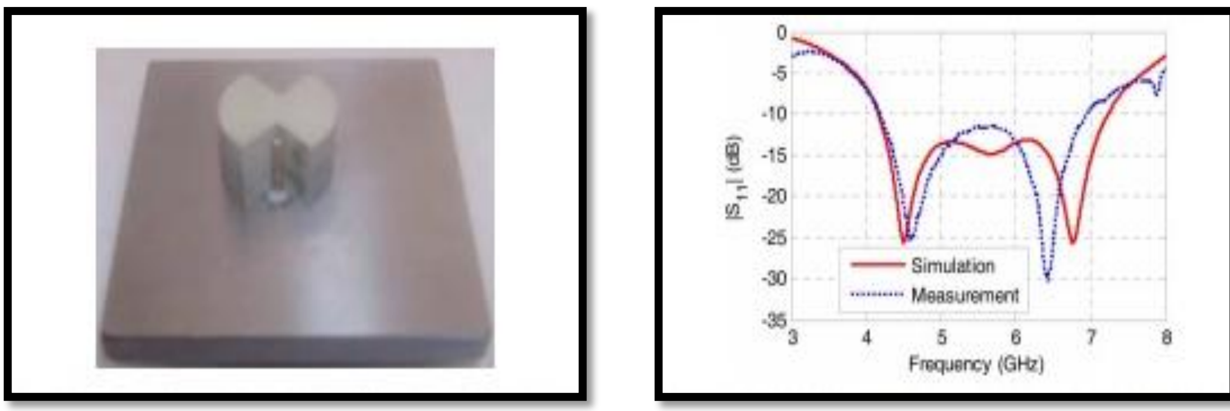

(a) **(b)**

Figure 1.9: (a) Photograph of optimized cylindrical Bowtie DRA prototype (b) Simulated and measured reflection for the cylindrical Bowtie DRA [45]

In 2015, Haque, Ahasanul, et.al; [46] Simulated return waste of the circular edge bow-tie nanoantenna is displayed in Figure (1-10) for various feeding line thickness. The recommended antenna presents better performance around the frequency of 25.3 THz with a feeding line thickness of 110 nm. it can be understood that the collected return loss value is below –10 dB in the range of 23.2 THz to 27 THz (bandwidth 3.8 THz) and from 31 THz to 35.9 THz (bandwidth 4.9 THz).

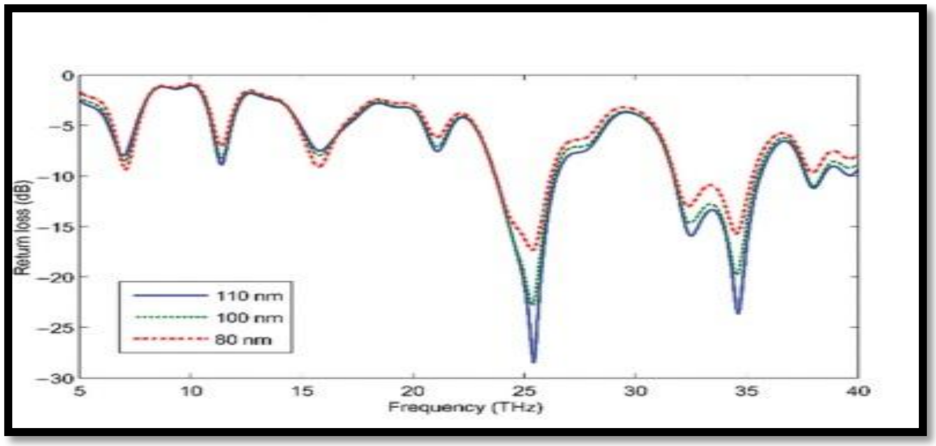

Figure 1**.10: Variation of the return loss versus frequency for different feeding line thickness [46]**

In 2016, Murad, Fadel A., et.al, [47] Presented the change of the electrical fields in the direction of propagation waves (x, y) respect to the length of an optical nanoantenna, that show approximately linear behavior, so, Decreasing the electric field in the gap for two electric fields in Y direction (Ey) and electric field in X direction (Ex) because of the increased surface area of the optical nanoantenna to increase the Length, which led to distribute charges over a larger area, and therefore leads to less concentration of Charges points of convergence as shown in the Figures (1-11, 1-12 and 1-13)[47].

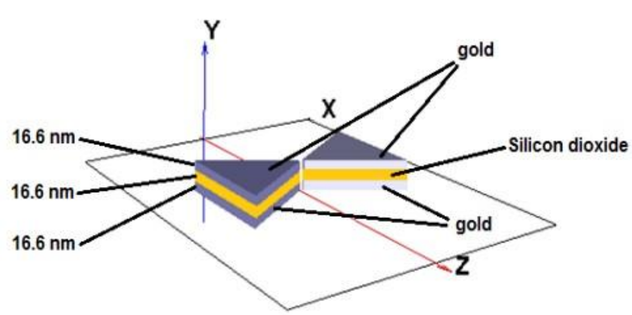

Figure 1.11 layer of optical nanoantenna according to propagation field[47]

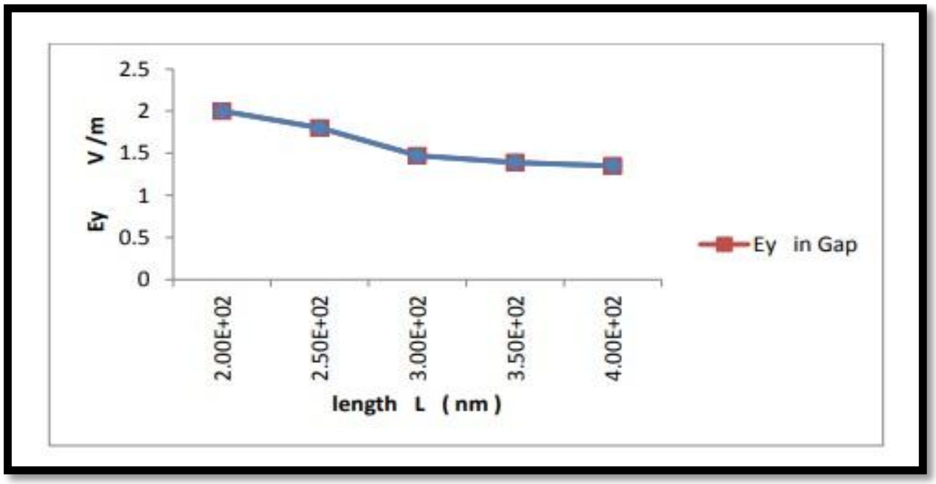

Figure 1.12: Electric field Ey Respect to the antenna lengths[47]

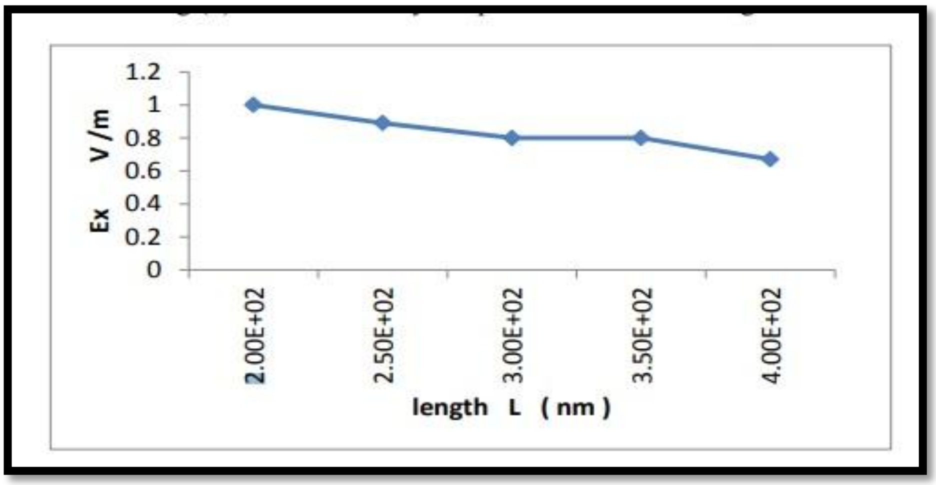

Figure 1.13: Electric field Ex Respect to the antenna lengths[47]

In 2017, Victor Pacheco-Peña, et.al; [48]: performed the design consists of a nanoantenna with two arms of angle θ, total length L=L1+L2 and the arms illuminated by a line dipole with arbitrary polarization. The gap between the two arms of (1 nm). He notices that high values of the electric field are obtained close to (35 dB). And in the coupling between the dipole nano-emitter and the Bowtie nanoantenna. The non-radiative Purcell improvement spectrum is estimated both analytically and numerically for various lengths, arm angles, and metals, demonstrating a good agreement between both procedures. The method here displayed fills the gap of the design techniques for optical nanoantennas.The design techniques for optical nanoantennas shown in Figure(1-14).

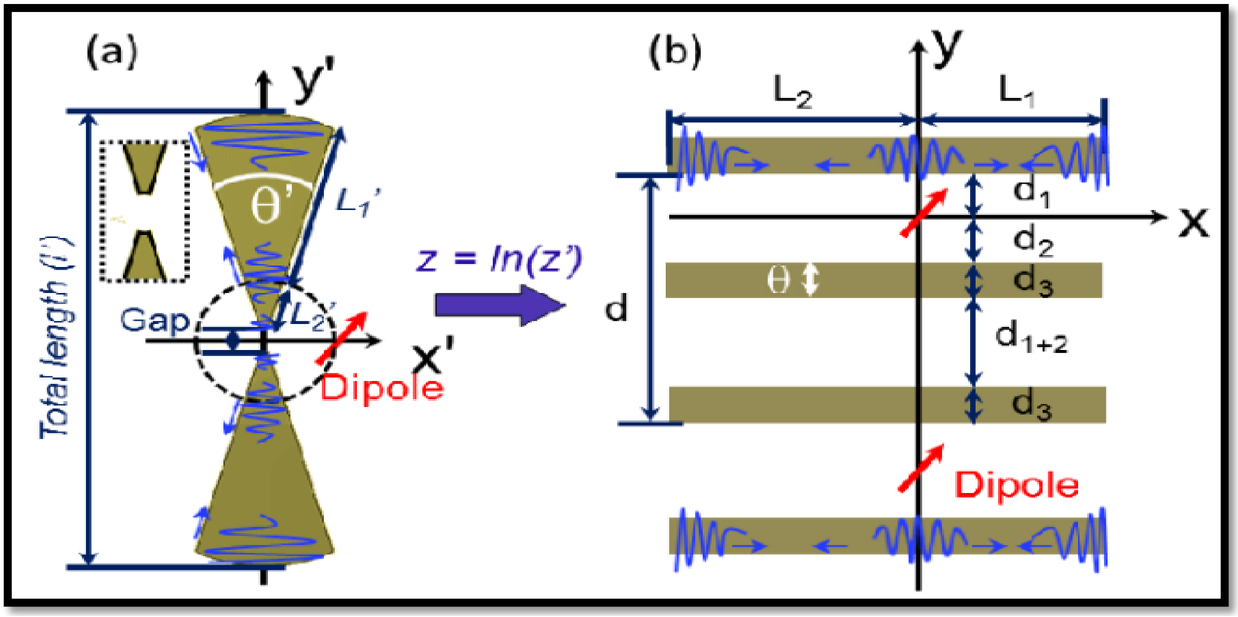

Figure 1.14: Bowtie nanoantenna under study (a) the transformed geometry (b) that consists of a periodic multi parallel plate geometry [48]

In 2018, Parul Goyal,et.al; [49]: A pair of hollow bow-tie nanoantenna with a feed gap has been designed utilizing gold in the visible frequency scale. This nanoantenna presents a great field improvement in the feed gap area at the resonance wavelength due to the localized surface plasmon. The absorption cross-section of this nanoantenna has been compared with the solid Bowtie nanoantenna and it has been remarked that the absorption cross-section in a hollow Bowtie nanoantenna is less as compared to a solid Bowtie nanoantenna. This is because of the less volume availability for light absorption in the hollow Bowtie nanoantenna. Therefore, the chief reason for utilizing a hollow Bowtie over a solid Bowtie is the reduced absorption cross-section. Moreover, characteristics of hollow Bowtie nanoantenna have been improved by geometric optimization utilizing COMSOL Multiphysics software.

CHAPTER TWO

MATERIAL AND METHOD

In this chapter, Nanoantenna has been submitted to investigate the influence of modifying the parameters of the nanoantenna such as (shape, material, thickness, the gap dimension), on the response of the nanoantenna such as far-field directivity, optical resonance frequency, and S-parameter. There are many kinds of nanoantenna have been investigated before, among these kinds is the Bowtie antenna. The influence of all nanoantenna parameters on the Bowtie nanoantenna response is studied.

The design is performed using a computer simulation technology (CST) studio.

Bowtie nanoantenna is formed with a pair of triangles nanoparticles realized in close nearness. This antenna is divided by a little gap to generate a greater electric field development in their gap area. This structure can be used for a biosensing application or SERS (surface-enhanced Raman spectroscopy) to develop recent discoveries and estimate the appearance of individual molecules. Thus, it is essential to build antennas with enough small gaps, to be able to compensate for the defects built through a fabrication process and reach antenna characteristics that are close to the ones forecast by simulations. Several kinds of beauty nanoantennas were experimented as shown in the literature, but we test a specific design of Bowtie nanoantenna with different geometries and materials .

2.1 Material and methods

In this work, we have used various materials in the design of Bowtie nanoantenna such as (gold, silver, aluminum,nickel, iron). The design was made using the (CST) program using (FIT) technique.

2.2 Design of the Bowtie Nanoantenna

Before starting to design an optical nanoantenna, the length of the optical nanoantenna, is assigned in the coordinate plane of the CST program (studio suite) and handled in the (FIT) method, where is inserted optical nanoantenna site by two points situated on the antenna axis which are in together ends of the optical nanoantenna (for each part). However, these two points situated at the peak of the triangle and the center triangle base, where between the two points will be the axis of symmetry of the triangle.

So, to painting a triangle that must set the position of these two points (end and start) are involved in both horizontal and vertical coordinates. The difference between Two Coordinate points is defined by a length of the rectum, which is painted a triangle, and When one of the coordinates of the two points are the same, that means:

1. Vertically (if the horizontal coordinates are equal)
2. Horizontally (if the vertical coordinates are equal)

For each of the two triangles are comparable to the two axes, as well as the axes are alike. Therefore, each horizontal dots for both triangles are equalized, the length of the optical nanoantenna is the difference between the farthest points of the vertical points, which are determining the length of the antenna. So, mathematically the optical nanoantenna length is the difference between Coordinates (Vertical < end) of the primary triangle and (vertical <end)of the second triangle. So, after analyzing the length of an optical nanoantenna, we have designed the optical nano antenna with a thickness of (20 nm) representing the total thickness of the constituent layers which consist of 2 layers (Gold Au - Silicon Si).

The first recommended antenna consists of flat edge bow-tie structure and the other side has tip (regular triangle) with a width Wa= (140 nm), thickness Ta=(20 nm), a length La= (130 nm) gap distance g=(10 nm), α= (64.94˚) and the material is (Gold) these nanoantenna are printed on a substrate Silicon (normal) Material as shown in Figure (2-1) set as a default type with:

ε= (11.9), μ = (1), Electric conductivity= (0.00025 S/m), ρ = (2330 kg/m^3), thermal conductivity = (148 W/K/m), thermal expansion = ($5.1\times 10^{-6}C^{-1}$) [51]. and with a width ws=(200 nm), length Ls=(290 nm), thickens Ts = (20 nm) as shown in Figure (2-1),

Electromagnetic Simulator is utilized for designing antennas formation and doing the numerical analysis. The recommended antenna was able to concentrate electric fields in the side of the substrate of the Bow-tie by a discrete port with incident frequency f= (0-700 THz). To use the explanation of boundary-value difficulties (a field problem) in engineering, the (FIT) method a computational procedure is utilized .

This antenna was designed for analyzing the electromagnetic radiations (far-field directivity, S -parameter, radiation pattern) which are studied with a linear polarized in this simulation. When applying numerical settling of Maxwell's equation in the electromagnetic simulation consider a great model mesh made critical law in simulation speed and precision.

So, the mesh grid (hexahedral) was estimated, where the mesh density was calculated by the size of the cell, and cells/wavelengths are read as twenty. However, the number of highest cell mesh was marked as (71.5657) and the number of cells is (21,120).

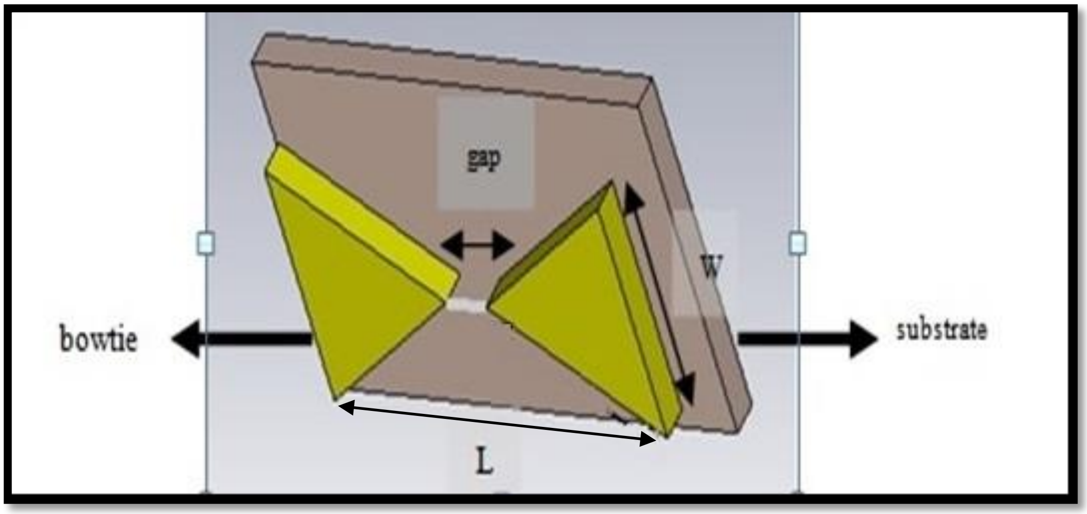

Figure 2.1: Bowtie nanoantenna

2.3 The material of Bowtie nanoantenna

In this part, the influence of changing the materials of nanoantenna was considered. The first way simulates the influence of the optical coefficients of the materials used. The second way considered the ability of the material to simulate. It considers the various material utilized in the design of Bowtie nanoantenna with a fixed of other parameters (length, gap distance, thickness).

For various material applied in a simulation design of Bowtie nanoantenna with width Wa=(140 nm), a length La= (130 nm), α=(64.94˚), thickness Ta=(20 nm), gap distance g=(10 nm), this nanoantenna are printed on a Silicon (normal) substrate with ws=(200 nm), Ls=(290nm) ,Ts = (20 nm) , the material used are (gold, nickel, silver, aluminum) , and the results were adjusted depending on the optical characteristics of the materials utilized.

2.4 The gap distance of Bowtie nanoantenna

By simulation of a bow tie nanoantenna with a length La= (130 nm), width Wa= (140 nm), α=(64.94°) ,thickness Ta=(20 nm), the gap distance is changed as g=(30,25,20,15,10,5), with (Gold a lossy metal) this nanoantenna are printed on a Silicon (normal) substrate with ws=(200 nm), Ls=(290nm) ,Ts = (20 nm) as shown in Figure (2.2). And the desired response parameters are S-parameter, resonance frequency.

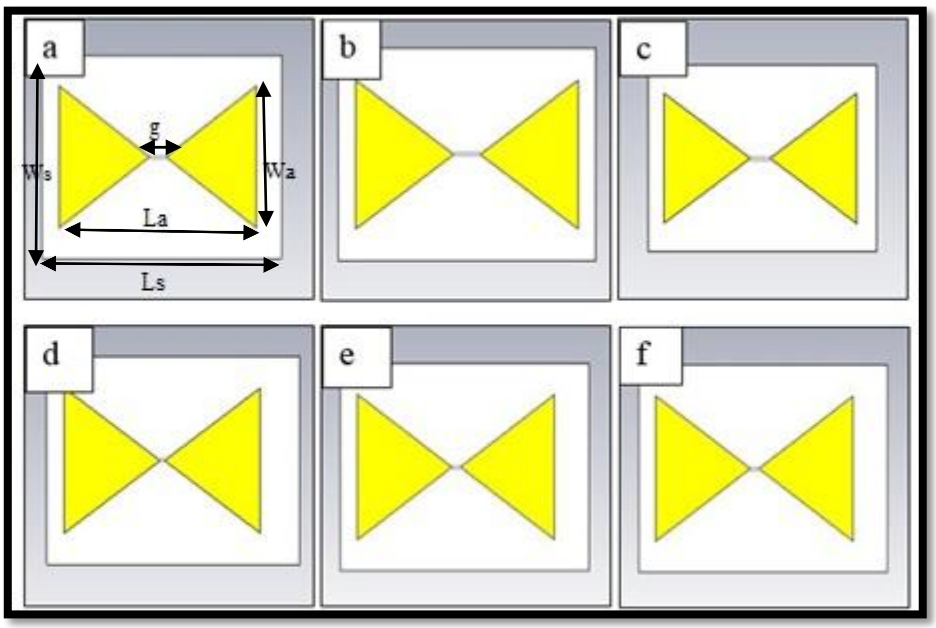

Figure 2.2 : With a Si substrate (a,b,c,d,e,f,) g=(30,25,20,15,10,5)nm

2.5 Design of Bowtie nanoantenna with a feeding

For antenna matching coditions to a certain frequency, feedings between the two nanoantenna arms become necessary. The antenna under test is a flat-edge Bowtie and made of aluminum and printed on the Si layer as a substrate, with the metal ground plane as a reflector, and a feeding structure placed in the gap of the

Bowtie antenna. The Drude model has been applied to studies the behavior of metal in the Terahertz frequency. The recommended antenna was designed utilizing 3D-electro-magnetic solvers (CST) programs and aimed for the thickness optimization of metals, geometrical length, and size of gaps. Simulations were conducted for investigation of the behavior of the illuminated nano-antenna by linearly polarized plane waves.

The numerical simulations are analyzed to enhance the most beneficial Electric-field of an antenna within the incident frequency light of (250–700 THz) frequency range. All results are shown in Chapter Three.

The recommended antenna is a flat-edged Bowtie aluminum structure; with length (La) = (141.42 nm), width (Wa) =(280 nm), thickness (Ta) = (50 nm), $\alpha = 90°$ and gap distance (g) = (50 nm). It was printed on a substrate of (silicon material) with: Ls=(280 nm), Ws= (360 nm), Ts = (100 nm). The Reflector is (Aluminum material): Lr = (280 nm), W r= (280 nm) Tr = (50 nm), and Aluminum material feeding in the gap of nanoantenna with Lf =(50 nm); Wf = (80 nm), Tf = (50 nm), as shown in Figure (2-3).

The electromagnetic simulator is utilized for designing the structure of the antenna and achieving numerical analysis. Moreover, the recommended antenna was able to concentrating the field at the side of the bootie with incident frequency light in tne range of (250–700 THz) .

This antenna shown in figure (2-3) is designed for studying electromagnetic radiation (far-field directivity), S parameter and resonance frequency which is analyzed with linear polarized plane waves, mesh grid (hexahedral) was deemed, where the mesh density was concluded using size of cell and the cells/wavelength was set to (20). However, the total number of cells in the mesh is (18,879).

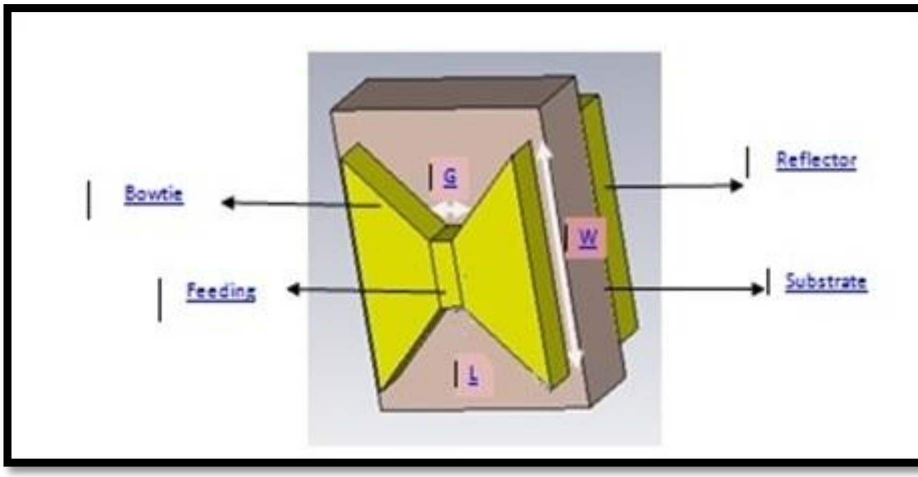

Figure 2.3: Flat-edge Bowtie nanoantenna

2.6 The material type of the feeding of flat-edge Bowtie nanoantenna

Simply, the feeding material (Gold, Silver, and Iron) is considered in this action. The influence of the change of these materials in the s11and resonance frequency and how discrete port current is changed according to the change in the material of the Bowtie nanoantenna are analyzed.

- Bowtie nanoantenna (Aluminum) material: La = (146.9 nm); Wa = (280 nm); $\boldsymbol{\alpha = 90}°$.
- Substrate silicone material: Ls=(280 nm), Ws = (360 nm), Ts = (100 nm)
- Reflector material (Aluminum): Lr=(280 nm), Wr =(280 nm), Tr =(50 nm)
- Feeding: Lf = (40 nm); Wf = (80 nm), Tf = (50 nm).

2.7 The feeding shape of Bowtie nanoantenna

In this step, the feeding shape is considered as shown in Figures (2-4),(2-5),(2-6), and the influence of changing these shapes on the response of nanoantennas is studied with the following parameters:

1) A rectangle feeding

- Bowtie nanoantenna (aluminum) material: La = (146.9 nm); Wa =(280 nm); $\boldsymbol{\alpha = 90}°$, gap = (40 nm); Ta = (50 nm).
- Substrate silicon material: Ls=(280 nm), Ws =(360 nm), Ts = (100 nm)
- Reflector (aluminum): Lr=(280 nm), Wr =(280 nm), Tr = (50 nm)
- Feeding aluminum material: Lf = (20 nm), Wf = (80 nm), Tf =(50 nm)

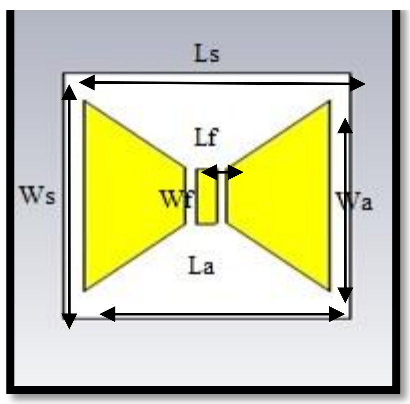

Figure 2.4: A rectangle feeding of flat-edge Bowtie nanoantenna

2) Spherical feeding

Changing the rectangle feeding to spherical feeding with a radius of (15, 10, 5) nm as shown in Figures (2-5; a, b, c) respectively for the nanoantenna with the same parameter above, and Aluminum made Bowtie nanoantenna.

- L a= (146.9 nm), W a=(280 nm), $\boldsymbol{\alpha = 90}°$, gap = (40 nm), Ta = (50 nm)

- Substrate Silicon material: Ls=(280 nm), Ws =(360 nm), Ts =(100 nm)
- Reflector (Aluminum): Lr=(280 nm), Wr =(280 nm) , Tr= (50 nm), and study the effect of these spheres on the responses of antennas

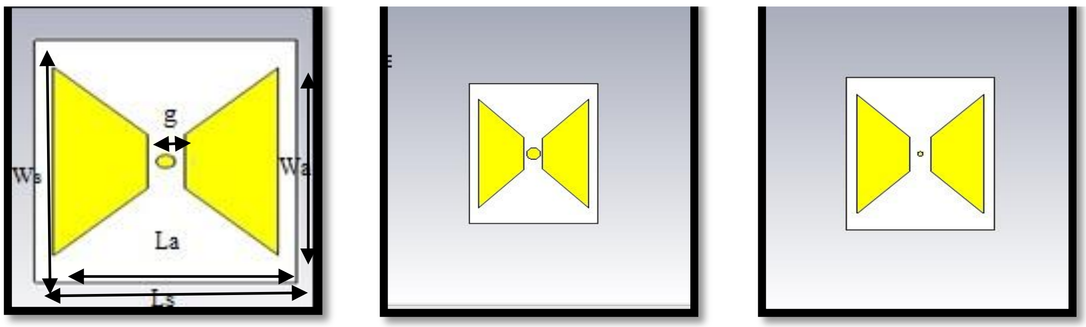

(a) (b) (c)

Figure 2.5: (a,b,c): A spherical feeding of flat-edge Bowtie nanoantenna

3) Three spherical feedings of Bowtie nanoantenna

A three (aluminum) spherical feedings of (10 nm) radius for each sphere are distributed in the gap of the nanoantenna as shown in Figure (2-6) while other parameter are the same as in the last design.

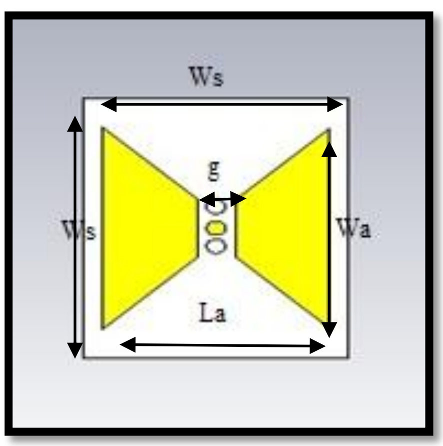

Figure 2.6: A three spherical feeding of flat-edge Bowtie nanoantenna

2.8 The material of three feedings of Bowtie nanoantenna

In this step, the material of three feedings was changed to Silver and fixed the other parameter

- Bowtie nanoantenna (Aluminum) material: La = (146.9 nm), Wa = (280 nm), $\alpha = 90°$, gap = (40 nm), Ta =(50 nm).
- Substrate silicon material: Ls=(280 nm), W s=(360 nm), Ts =(100 nm).
- Reflector (Aluminum): Lr=(280 nm), Wr =(280 nm), Tr =(50 nm).

As shown in Figure (2-7) and study the effect of these changes on the response of nanoantenna.

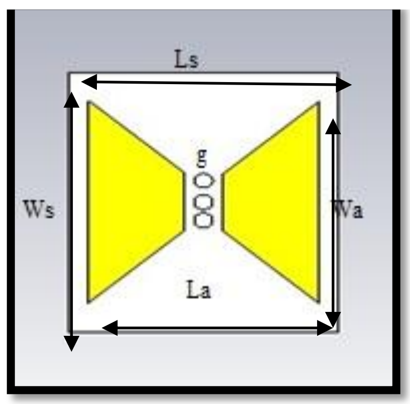

Figure 2.7: A three silver spherical feeding of flat-edge Bowtie nanoantenna

2.9 The feeding type of Bowtie nanoantenna

1) With air feeding

Here the feeding is air in the gap of the Bowtie nanoantenna (Aluminum) and the other parameters are fixed at:

- nanoantenna (Aluminum) material La = (141.4 nm), W a= (200 nm),

$\alpha = 90°$; Ta =(50 nm).

- Dielectric substrate silicone material: Ls = (200 nm) Ws = (360 nm), and Ts = (40 nm).
- Reflector Aluminum material: Lr=(280 nm), Wr = (280 nm), Tr = (50 nm) Gab L = (10 nm) as shown Figure (2-8).

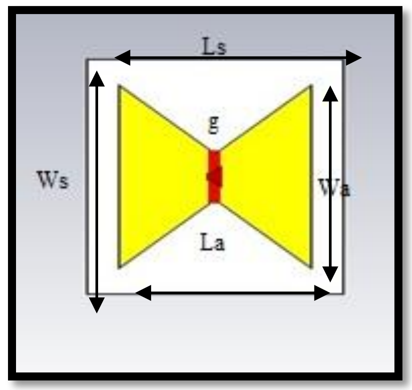

Figure 2.8: flat-edge Bowtie with air feeding

2) <u>The dielectric feeding</u>

In this step, the feeding is a dielectric material and other parameters are fixed at:

- Bowtie nanoantenna (Aluminum) material:(La = 141.4 nm) Wa = (200 nm) $\alpha = 90°$; Ta = (50 nm).
- Dielectric Substrate Silicon material: Ls = (200 nm) Ws = (360 nm), Ts = (40 nm)
- Reflector Aluminum: Lr=(280 nm), Wr =(280 nm), Tr = (50 nm)
- Gab is dielectric: L f= (10 nm) as shown in Figure (2-9).

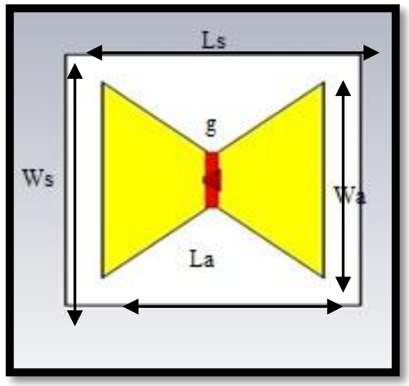

Figure 2.9: flat-edge Bowtie nanoantenna with a dielectric feeding

2.10 Three spherical feeding in the gap of flat-edge Bowtie nanoantenna

The reflector was removed from the flat-edge Bowtie nanoantenna and the other parameters of nanoantenn are fixed at:

- Bowtie nanoantenna (Aluminum) material: La = (146.9 nm); Wa = (280 nm); $\boldsymbol{\alpha = 90}$°, gap =(40 nm); Ta =(50 nm)
- Substrate Silicon material: Ls =(280 nm); Ws =(360 nm); Ts =(100 nm)

Three feeding materials of Aluminum with a radius (10 nm) are used as shown in Figure (2-10).

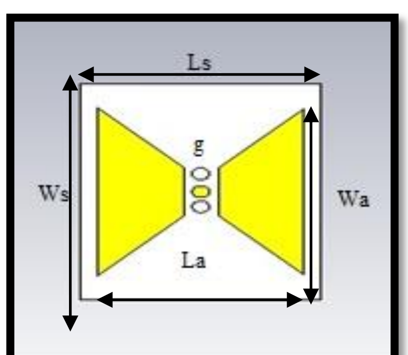

Figure 2.10: A flat edge of Bowtie nanoantenna with out reflector

CHAPTER THREE

Result, Discussion, and conclusion

In this chapter, the results of various designs of the Bowtie nanoantenna of ch.2 are reported and concluded. Depend on broadband calculations in the near-infrared and noticeable range of the visual spectra performed within the technique of finite integration, we center our study on such nanoantenna's far-field optical characteristics, the directivity, s-parameter (reflection coefficient) and resonance frequency. A detailed and systemic demonstration of the influences is obtained in the current work for the idea of the design of the nanoantenna. These bow-tie nanoantennas can be easily linked with microscopes to produce a powerful light spot for sufficient illumination when probing the near-field characteristics in the microscopy.

3.1 Effect of the parameters of the Bowtie nanoantenna

In our research, we studied the effects of the parameters of the Bowtie nanoantenna such as (gap distance, thickness of the Bowtie nanoantenna, the material of the Bowtie nanoantenna) on the response of Bowtie nanoantenna and the results are as follows:

3.2 Gap distance effect

Because of a localized surface Plasmon excitation, the variation of the gap distance between the two nanostructures can control the improvement of the electric field around the gap, the resonance frequency, and s-parameter. Table (3.1) shows the response of Bowtie nanoantenna with Si substrate.

Table 3.1: The resonance frequency, S-parameter response for Bowtie nanoantenna shown in fig.(2.2)with a Si substrate and with a different values of gap distance

Gap nm	**S-parameter dB**	**Resonance frequency THz**
30	-16.9	310.23
25	-17.8	320.45
20	-19.11	330.68
15	-20.97	343.18
10	-24.1	356.82
5	-33	377.3

From the table (3-1), the s- parameter at a small gap is higher than that of big gap, and the resonance frequency increased with decreasing the gap width. However , reducing the gap between Bowtie triangle, the coupling will result in a blue shift of the coupling mode which match the results in [54]. And changing the gap leads to multiple local resonances which effects S-parameter (return losses) in agreements with work of [55].

Figures(3-1;a,c,b,d,f,e) show results of the s-parameter of Bowtie nanoantenna with a silicon substrate shown in Figure (2-1) when changing the gap distance g= (30,25,20,15,10,5) nm respectively as shown in Figure (2-2).

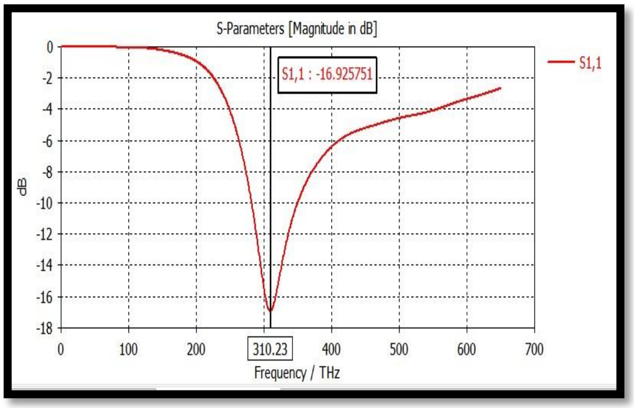

(a) S-parameter of Bowtie nanoantenna with g= (30) nm

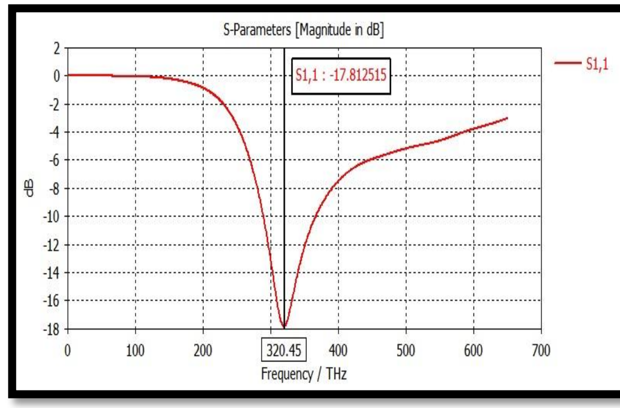

(b) S-parameter of Bowtie nanoantenna with g= (25) nm

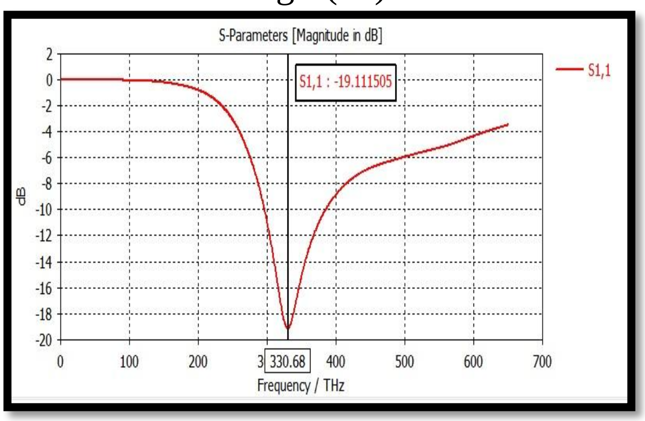

(c) S-parameter of Bowtie nanoantenna with g= (20)nm

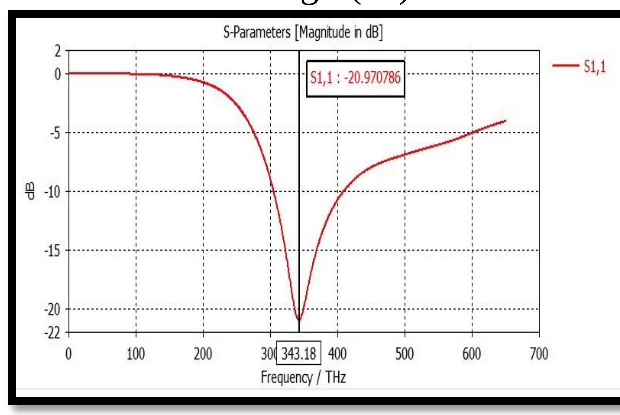

(d) S-parameter of Bowtie nanoantenna with g= (15) nm

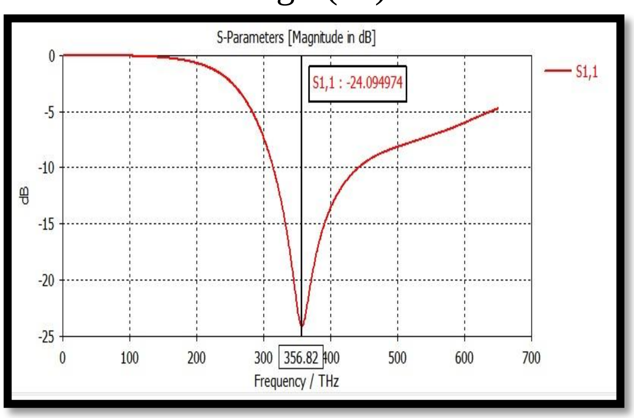

(e) S-parameter of Bowtie nanoantenna with g= (10) nm

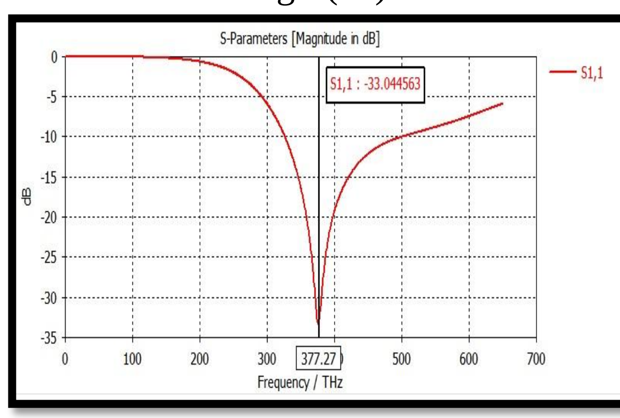

(f) S-parameter of Bowtie nanoantenna with g= (5) nm

Figure 3.1 :Figs. (a,b,c,d,e,f,) show s-parameter and resonance frequency for Bowtie nanoantenna shown in fig.(2.1)with a silicon substrate and different values of gap distance

There is a relation between the gap, s-parameter, and resonance frequency as shown in Figure (3-2) for Bowtie shown in Figure (2-1) with Si substrate.

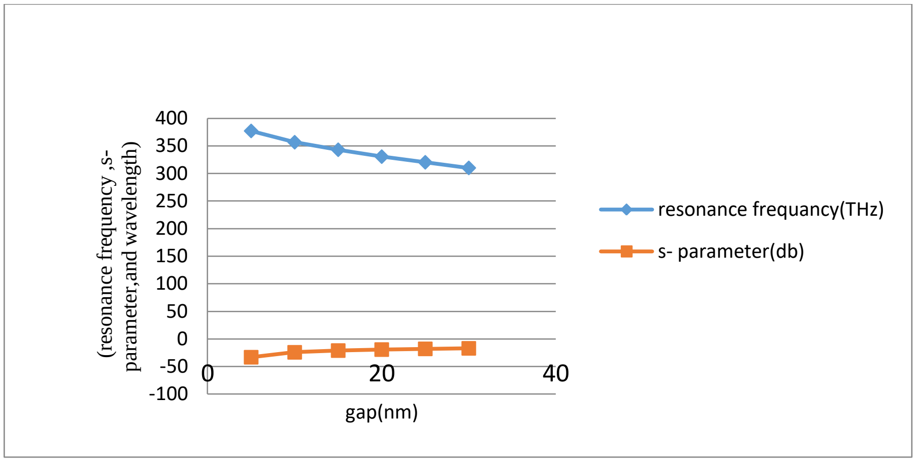

Figure 3.2: Effects of the gap for Bowtie nanoantenna shown in Fig.(2.1)with a silicon substrate and different values of gap on the (resonance frequency, s- parameter,)

, the blue curve is for the resonance frequency in THz, and the red curve is for s-parameter in dB. The result shows that the increase of the gap dimension leads to decrease the resonance frequency and the s- parameter is maximized. These results are matched with results of reference [54,58].

3.3 The Material effect of of Bowtie nanoantenna

In this section, the effect of the material of the nanoantenna shown in Figure (2-1) on the resonance frequency, and s-parameter was studied. Different materials are used in the design of Bowtie nanoantenna while other parameters (length, gap distance, thickness) are not altered. The results were shown in the table (3-2).

Table 3.2: The resonance frequency, S-parameter response for Bowtie nanoantenna shown in fig.(2.1)with Si substrate and with different Bowtie materials

Material	**S-parameter dB**	**Discrete port current**	**Resonance frequency THz**
Gold	-23.4	-17.053	367
Nickel	-6.23	-28.1	145.4
Silver	-30.4	-16.91	369.4
Aluminum	-33.6	-16.98	367

Different materials ; Aluminum, Gold, Silver and Nickel are used in a simulation design of Bowtie nanoantenna with the Si substrate as shown in figure (3-5) (a,b,c,d) for discrete port current. Table (3-2) show the resonance frequency, S- parameter response discrete port current. The results were changed depending on the optical properties of the materials used. The Gold shows best s-parameter (-23.4 dB) and resonance frequency of (367 THz). While when using Nickel material, the s- parameter was (-6.23dB), this various result, can be understood in term of directivity and skin depth of metal, the large skin depth leads to shifting to the lower frequency, and the amplitude of the impedance depends on the conductivity of the material as described in reference [56,60]. The lower dc conductivity leads to high metal impedance. As shown in the result of the nickel. So, it is very important to choose the proper material in the design to get good efficiency of the Bowtie nanoantenna.

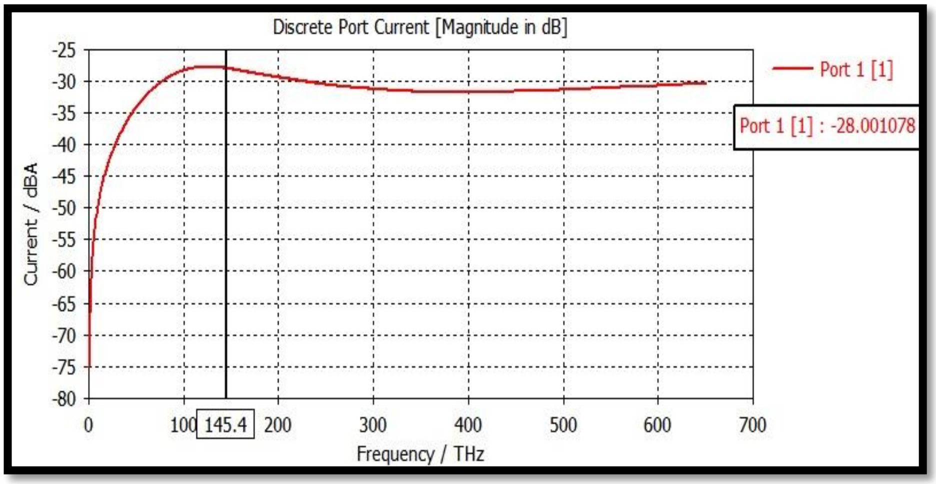

(a): Current (dB) vs. Frequency (THz) for Nicle nanoantenna

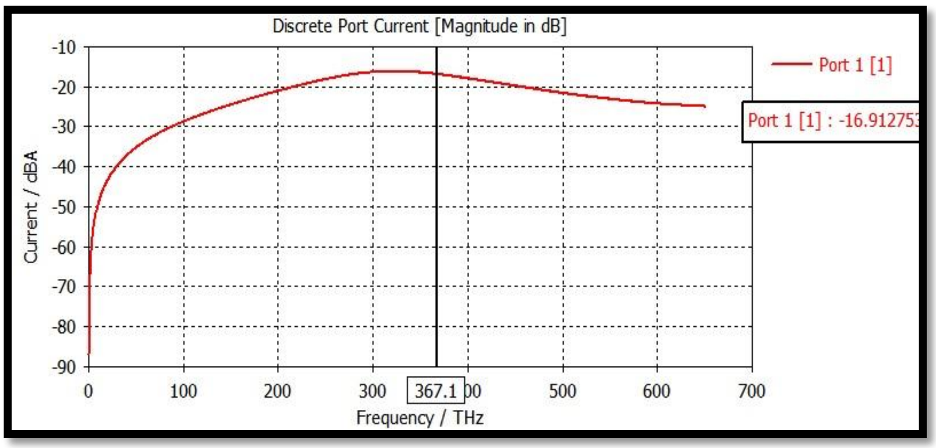

(b): current (dB) vs frequency (THz) for aluminum nanoantenna

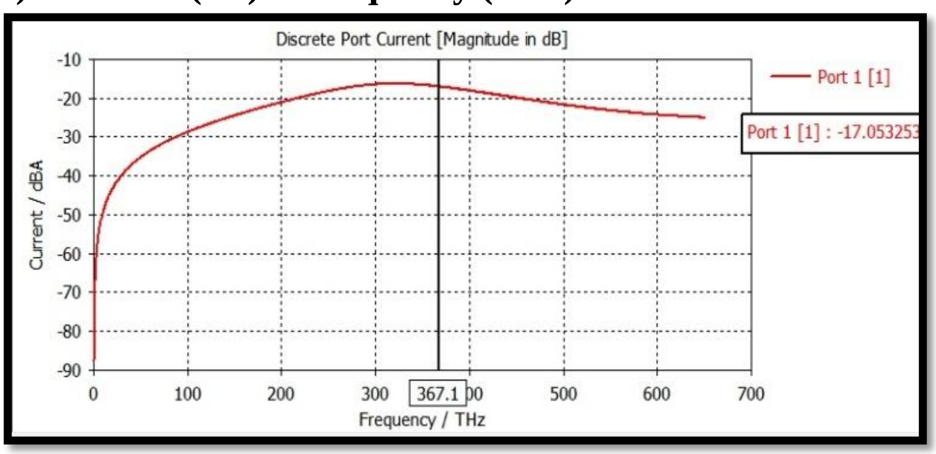

(c) : Current (dB) vs. frequency (THz) for Gold nanoantenna

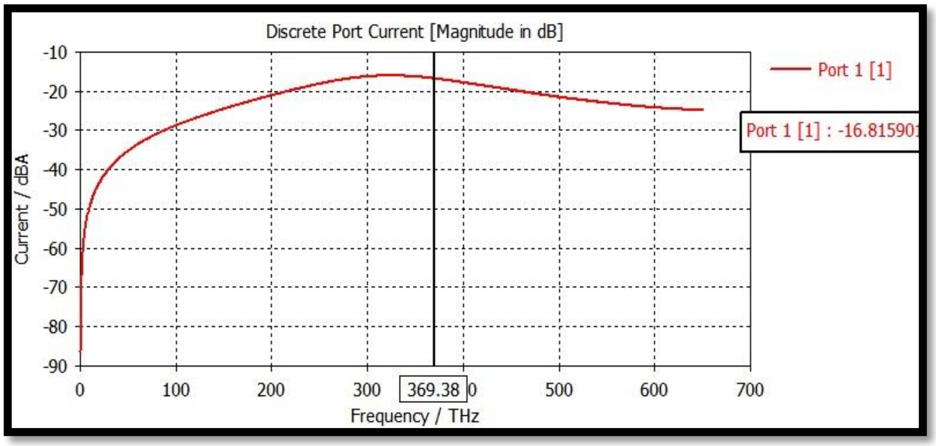

(d): Current (dB) vs. frequency (THz) for Silver nanoantenna

Figure (3.3;a,b,c,d) results of discrete port current with resonance frequency for different Bowtie materials with Si substrate

3.4 Effect of the radiation pattern of the far field of Bowtie nanoantenna

The radiation pattern_of Bowtie nanoantenna which shown in Figure (2-1) , is shown in Figure (3-4) with a Si substrate The Bowtie antenna has a (donut) form radiation pattern, along the z-axis. Which show maximum power in the x-y plane which agree with results in [58-59].

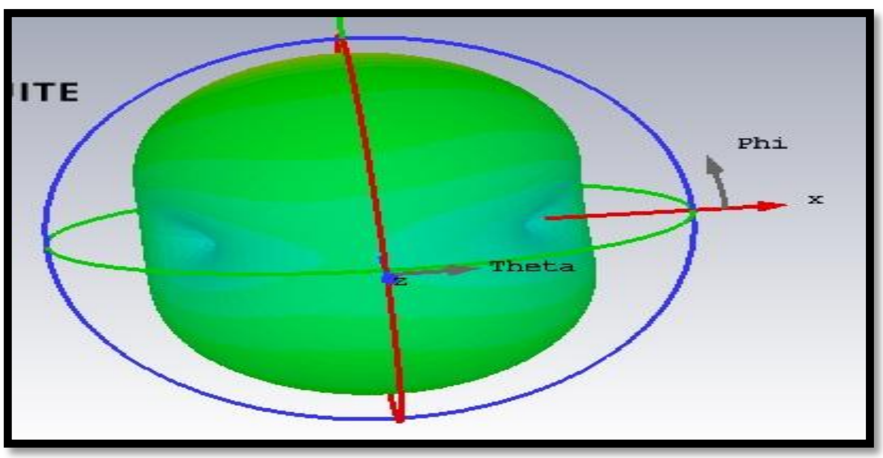

Figure 3.4: 3-d radiation pattern for Bowtie nanoantenna shown in figure (2.1) with a silicon substrate

The far-field directivity of this Bowtie nanoantenna was calculated as shown in the Figure (3-5) for Bowtie with Si substrate.

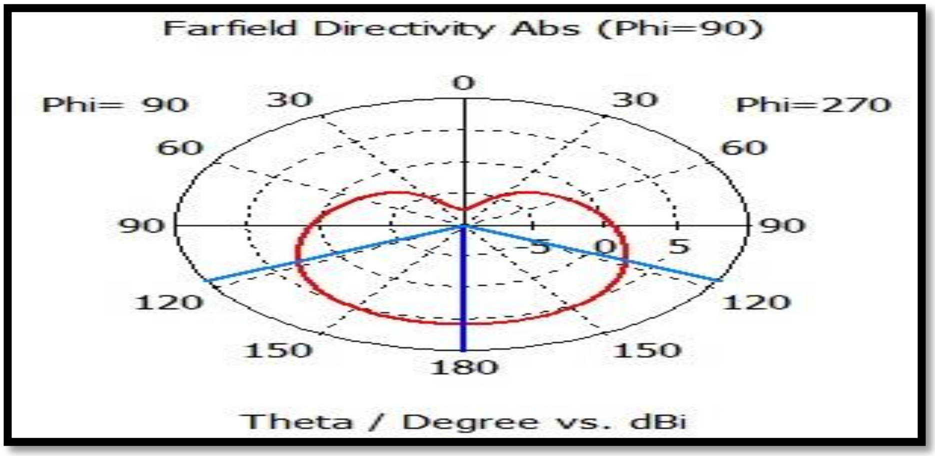

Figure (3.5): Far-field directivity for Bowtie nanoantenna shown in Figure (2.1) with a silicon substrate

The red curve stands for Eθ $pattern$ $(\theta)$is the angle between the z-axis and the vector from the origin to the point (ranges from 0 to180 degrees), the blue lines represent the half-power bandwidth (the angle encompassed between the points on the side of the lobe where the power has fallen to half (-3dB) of its maximum value) and the green curve is the magnitude of the back loop(usually represent the side lobe in opposite direction from the main lobe) [57]. In this study, the gap size plays a useful role in capturing electric fields.

As it was seen in Figure (3-5), for Bowtie with Si substrate, the main lobe magnitude is 3.19dB, and the Main lobe direction is180 deg.

Sometimes the antennas are omnidirectional which have isotropic radiation pattern in a single plane so, a Bowtie antenna is an omnidirectional pattern in agreement with [59,60]. And It shows a half-power bandwidth obtained at a frequency (650 THZ) by simulation of the optical Bowtie nanoantenna with Si substrate.

3.5 Effect of the feeding material of a flat-edge Bowtie nanoantenna

The materials of feeding and Bowtie were changed (gold, silver, iron, and aluminum) for nanoantenna shown in Figure (2-3) in chapter 2. The influence of changing the materials of Bowtie and feeding on the S11, resonance frequency and discrete port current were studied. The results are shown in table (3-3).

Table 3.3: The resonance frequency, S-parameter response for a flat-edge Bowtie nanoantenna shown in fig.(2.3) with different feeding and Bowtie materials

Material(Bowtie and feeding)	s-parameter dB	Discrete port current	Resonance frequency THz
Gold	-9.07011	-19.74669	301.87
Silver	-9.567	-19.65	301.73
Iron	-7.50657	-20.128	302.45
Aluminum	-8.812439	-19.70212	302.46

When using silver material the s-parameter is the best (-9.567 dB) and resonance frequency (301.73 THz) and the iron is the lowest result of s-parameter (-7.506 dB), and resonance frequency(302.45 THz) . Figures (3-6;a,b,c,d,e,) show the results of discrete port current and resonance frequency for these materials (gold, silver, iron, and aluminum).

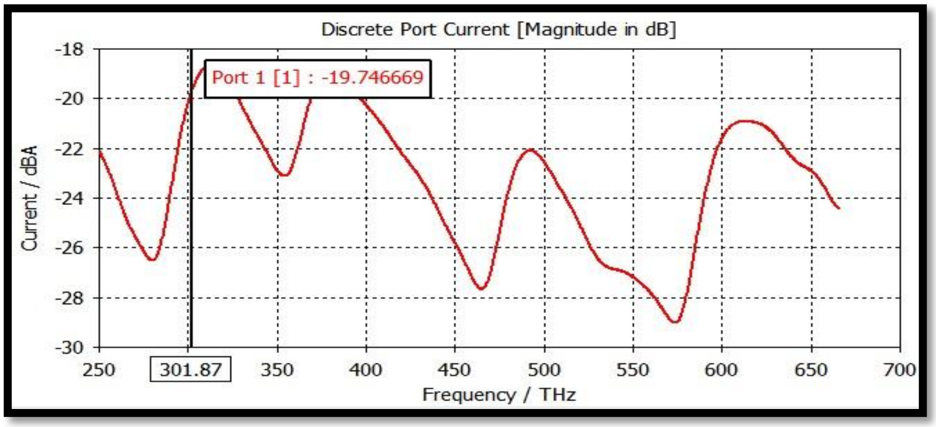

(a) discrete port current with resonance frequency for Gold Bowtie nanoantenna

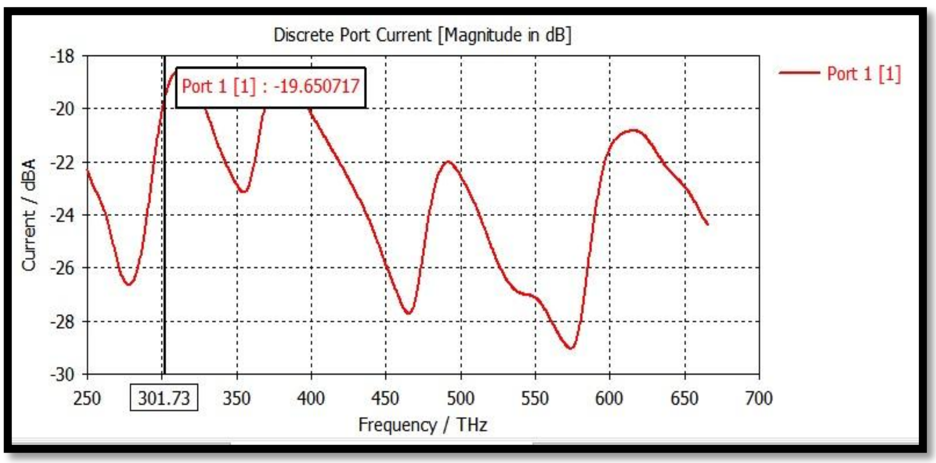

(b) discrete port current with resonance frequency for Silver Bowtie nanoantenna

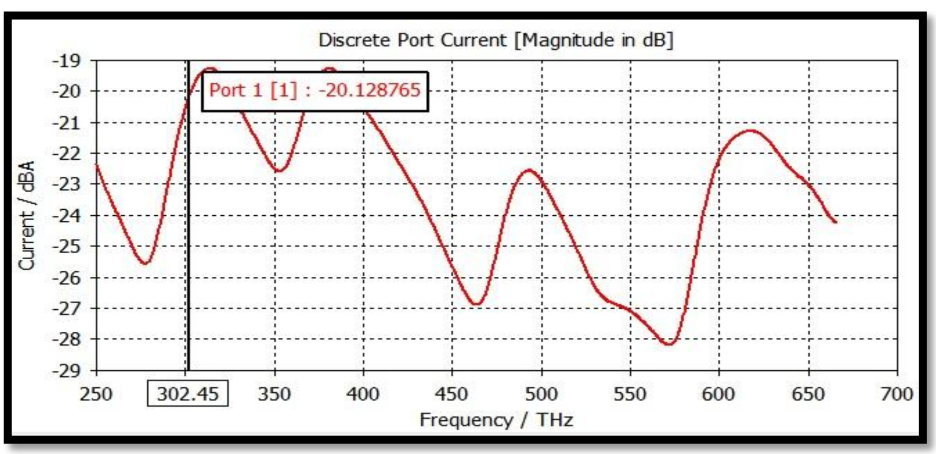

(c) discrete port current with resonance frequency for iron Bowtie nanoanten)

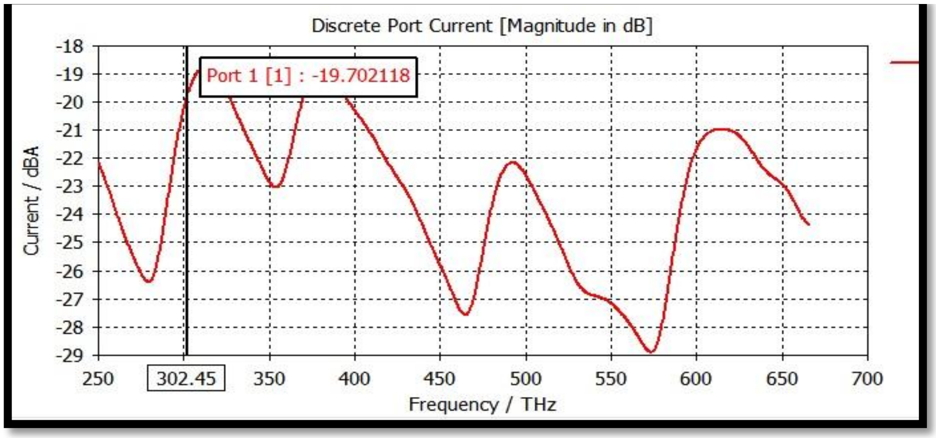

(d) discrete port current with resonance frequency for Aluminum Bowtie nanoantenna

Figure 3.6: (a,b,c,d) results of discrete port current with resonance frequency frequency for different Bowtie and feeding materials

3.6 Effect of A rectangle feeding of flat-edge Bowtie

Figure (3-7),(3-8) shown the result of S-parameter and 3d pattern for A flat-edge Bowtie nanoantenna when the feeding length is changed from(40nm) to (20nm) as shown in Figure (2-4), the Feeding is aluminum material: L = (20 nm), W = (80 nm), T = (50 nm).

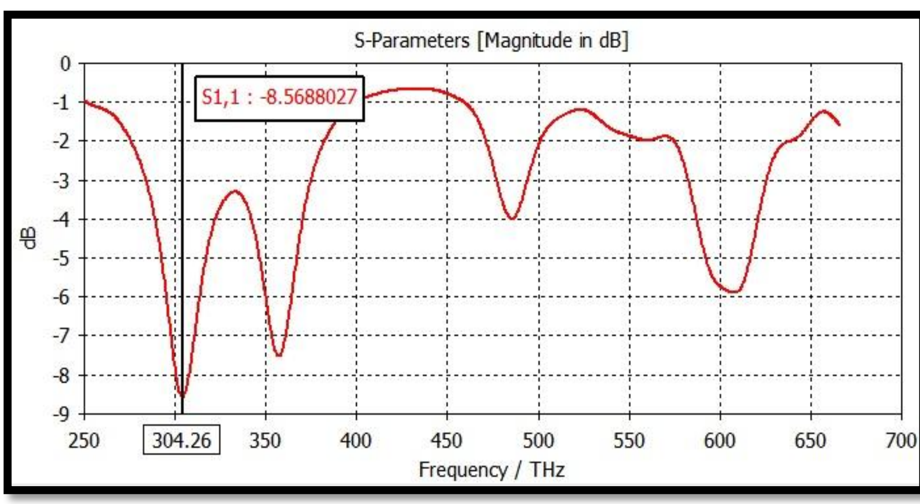

Figure 3.7: The results of s- parameter and resonance frequency of flat-edge Bowtie nanoantenna in fig (2.4) when using an (aluminum) rectangle feeding

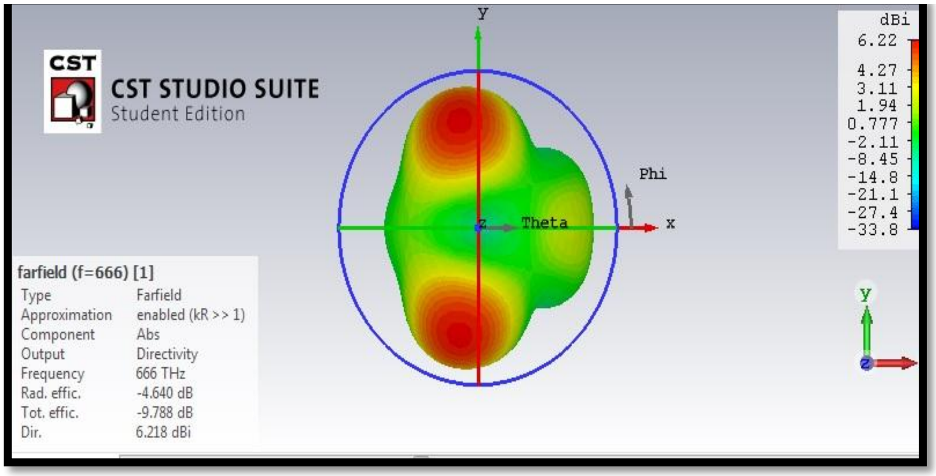

Figure 3.8: 3D pattern directivity of flat-edge Bowtie nanoantenna in fig (2.4) when using an (aluminum) rectangle feeding

From Figure (3-7) and figure (3-8), the S-parameter is found to be (-8.6 dB) at a resonance frequency of (304.3 THz), and the directivity is(6.215) at an incident light frequency of(666 THz).

3.7 Effect of using a spherical feeding of flat-edge Bowtie nanoantenna with a radius of (15 nm)

In these steps, the effects, spherical feeding with a radius of (15 nm) for the nanoantenna which is shown in Figure (2-5)a, is illustrated in Figure (3-9) and Figure (3-10).

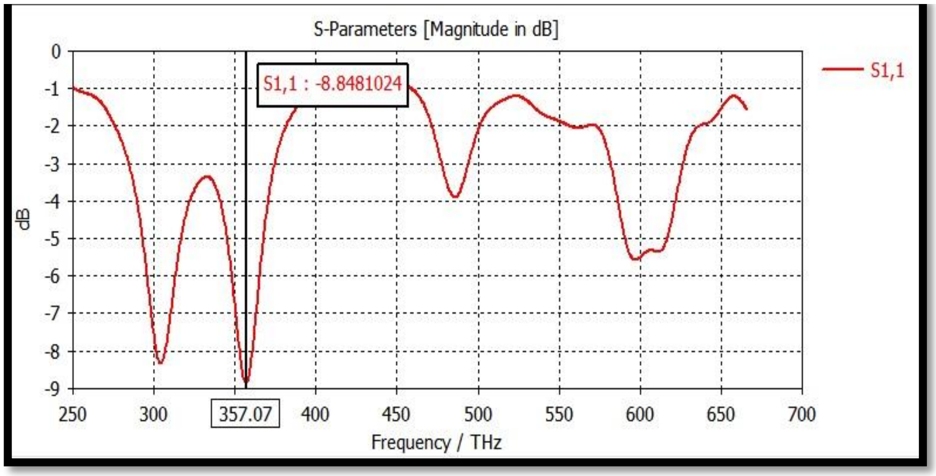

Figure 3.9: The results of S-parameter and resonance frequency for flat-edge Bowtie nanoantenna of fig (2.5)a when using an (aluminum) spherical feeding with a radius of(15 nm)

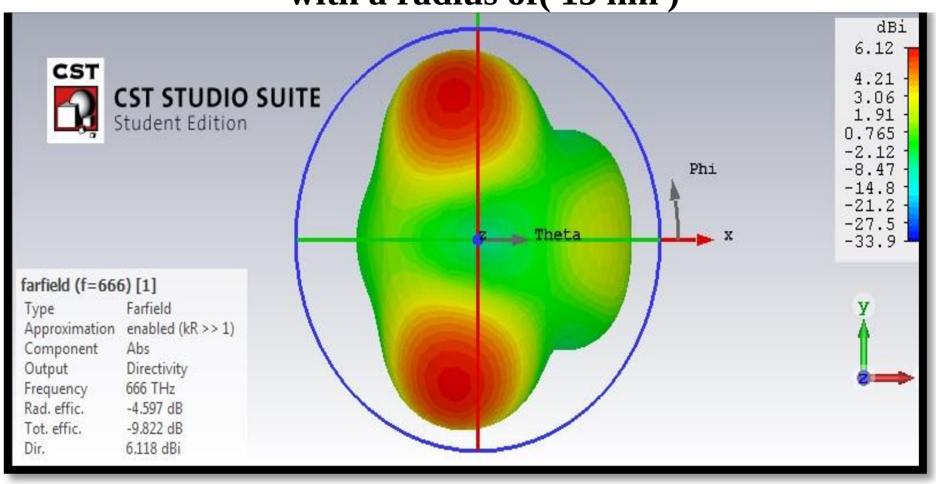

Figure 3.10: 3D pattern directivity of flat-edge Bowtie nanoantenna shown in fig(2.5)a when using an (aluminum) spherical feeding with a radius of. (15nm)

From Figure (3-9) and figure (3-10), the S-parameter is found to be (-8.85 dB) at a resonance frequency of(357.5 THz), and the directivity is(6.1) at an incident frequency of (666 THz).

3.8 Effect of Changing the radius of spherical feeding of flat-edge Bowtie nanoantenna to (10 nm)

In this step, the radius of spherical feeding is (10 nm) for the nanoantenna shown in Figure (2-5) b, and the results are exhibited in Figure (3-11) and Figure (3-12).

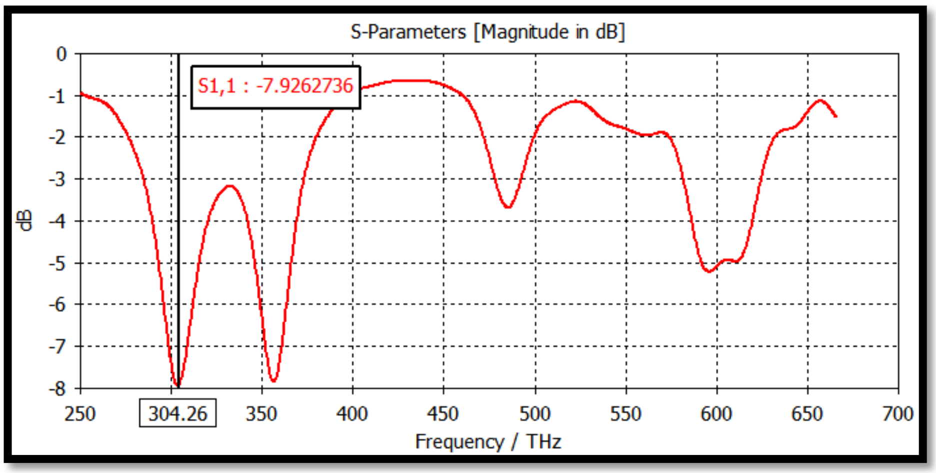

Figure 3.11: S-parameter and resonance frequency for flat-edge Bowtie nanoantenna of fig (2.5)b when using an (aluminum) spherical feeding with a radius of(10 nm)

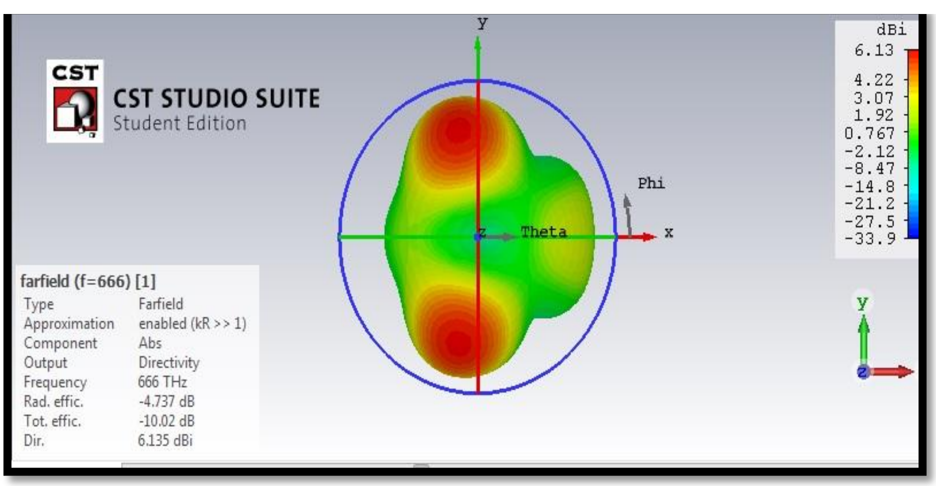

Figure 3.12: 3D pattern directivity of flat-edge Bowtie nanoantenna of fig(2.5)b when using an (aluminum) spherical feeding with a radius of. (10 nm)

From Figure (3-11) and Figure (3-12), the S-parameter is found to be (-7.9 dB) at a resonance frequency of (304.3 THz), and the directivity is (6.1) at an incident frequency of (666 THz).

3.9 Effect of Changing the radius of the spherical feeding of flat-edge Bowtie nanoantenna to (5nm)

In this step, feeding sphere radius is (5 nm) for the nanoantenna shown in Figure (2-5) c and results are exhibited in Figure (3-13) and Figure (3-14).

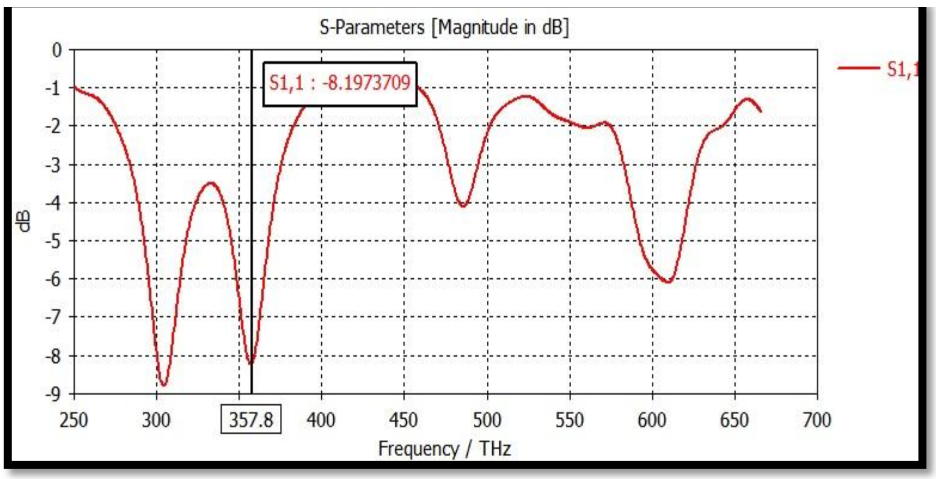

Figure 3.13: S-parameter and resonance frequency of flat-edge Bowtie nanoantenna in fig(2.5)c when using an (aluminum) spherical feeding with a radius of(5 nm)

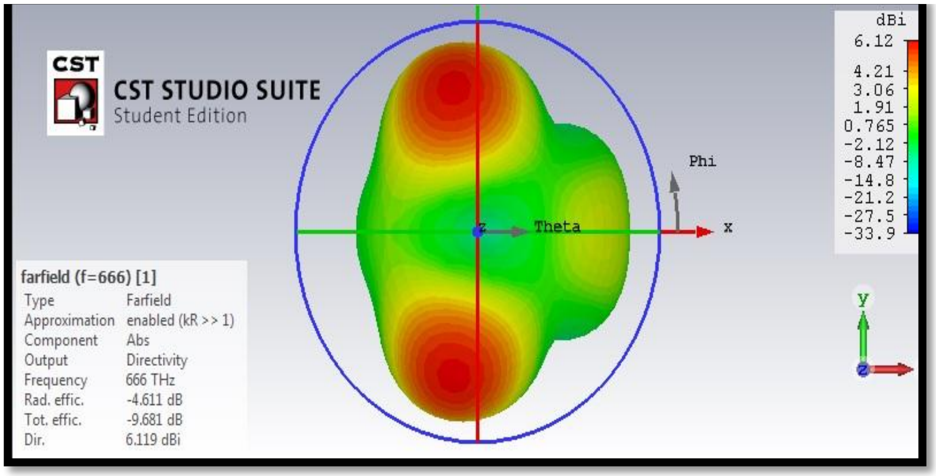

Figure 3.14: 3D pattern directivity of flat-edge Bowtie nanoantenna in fig(2.5)c when using an (aluminum) spherical feeding with a radius of. (5 nm)

From Figure (3-13) and Figure (3-14), the S-parameter is found to be (-8.2 dB) at a resonance frequency of (358THz), and the directivity is (6.12) at an incident frequency of (666 THz).

3.10 Effect of using Three spherical feedings of flat-edge Bowtie nanoantenna

In the nanoantenna shown in Figure (2-6) in chapter 2, three spherical feedings of aluminum material are used. The results are seen in Figure. (3-15), Figure (3-16), and Figure. (3-17), for the s- parameter is (-8.9 dB) at the resonance frequency of(303.5 THz), and the directivity is (6.17).

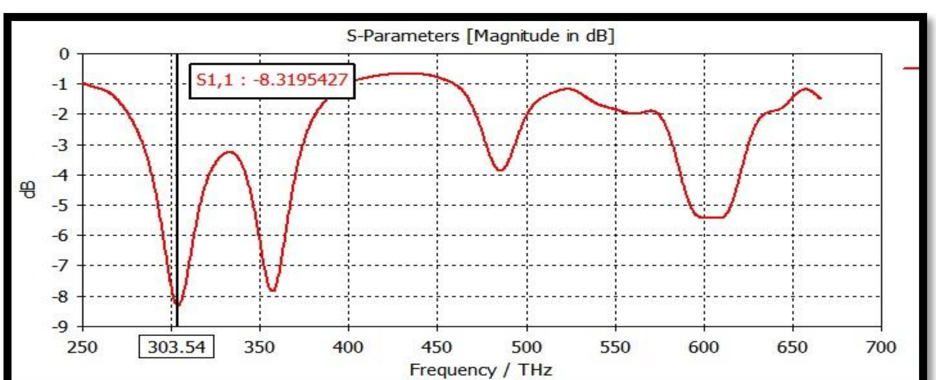

Figure 3.15: The results of S-parameter and resonance frequency of flat-edge Bowtie nanoantenna in fig (2.6) when using an (aluminum) three spherical feeding with a radius of (10 nm)

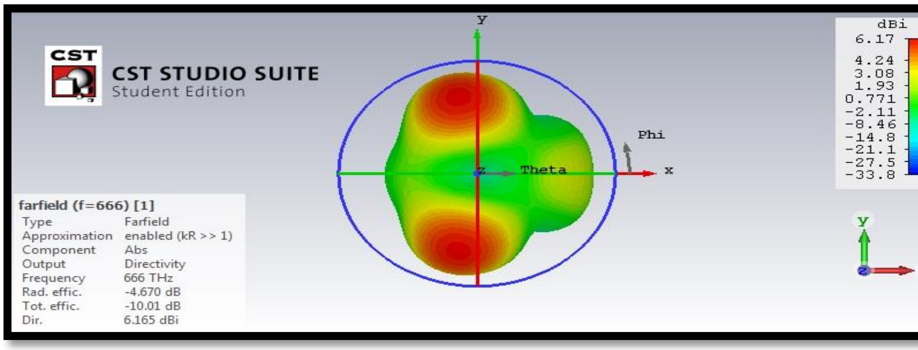

Figure 3.16: 3D pattern directivity of flat-edge Bowtie nanoantenna in fig (2.6) when using an (aluminum) three spherical feeding with a radius of (10 nm)

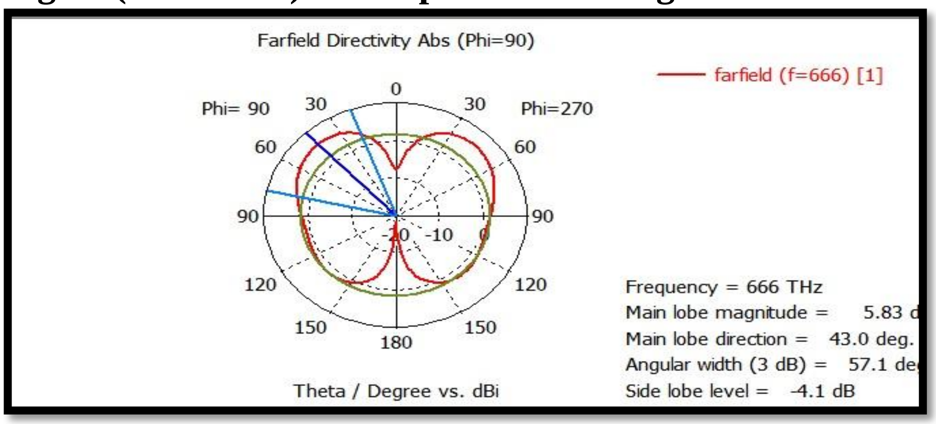

Figure 3.17: The polar plot of flat-edge Bowtie nanoantenna in fig (2.6) when using an (aluminum) three spherical feeding with a radius of (10 nm)

3.11 Effect of Change the material of three feedings of flat-edge Bowtie nanoantenna

For the nanoantenna shown in Figure (2-7), the material of the sphere feeding used is silver material. The results are as shown in Figure (3-18), Figure (3-19) and Figure (3-20), for the s- parameter is(-8.32 dB), at the resonance frequency of (303.5 THz),and the directivity is (6.16)

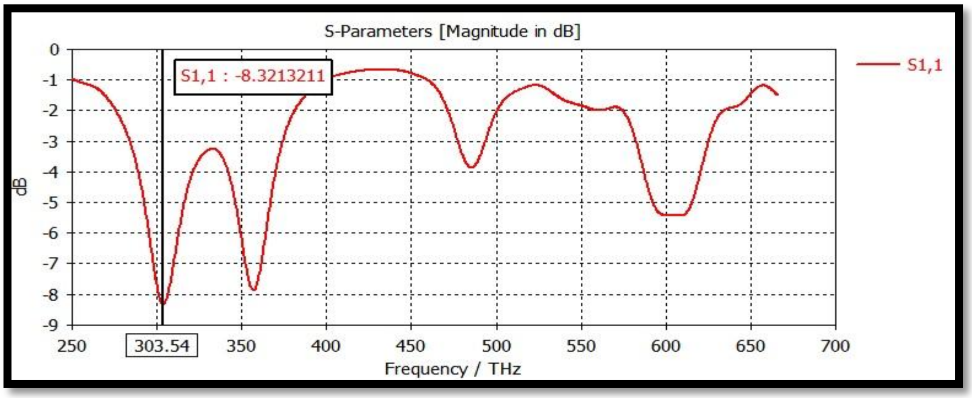

Figure 3.18: S-parameter and resonance frequency of flat-edge Bowtie nanoantenna in fig (2.7) when replacing the material of the three spherical feeding to Silver

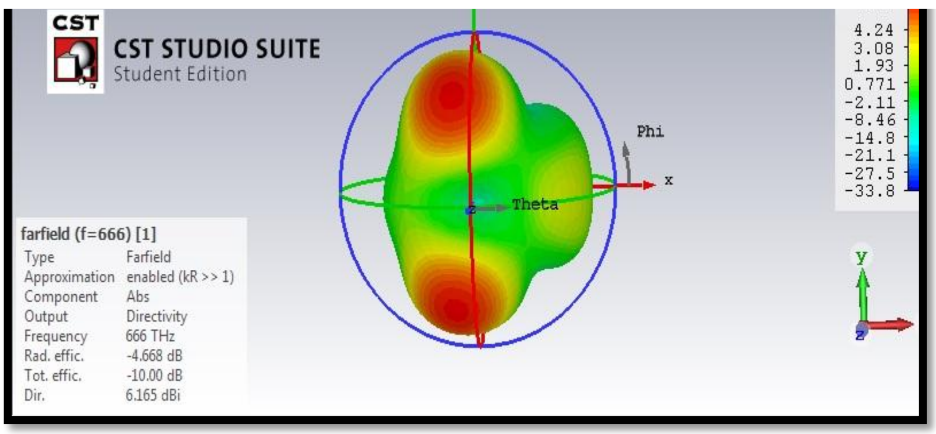

Figure 3.19: The 3-d radiation pattern of flat-edge Bowtie nanoantenna in fig (2.7) when replacing the material of the three spherical feeding to Silver

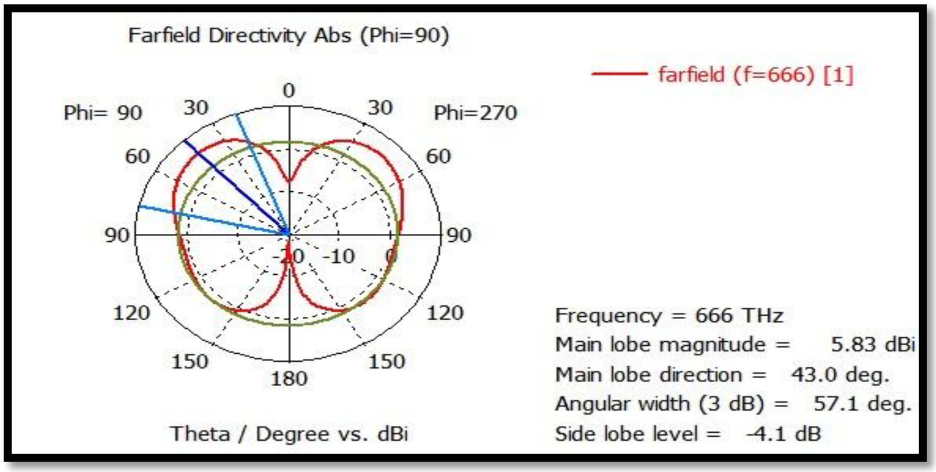

Figure 3.20: The polar plot of flat-edge Bowtie nanoantenna in fig (2.7) when replacing the material of the three spherical feeding to Silver

3.12 Effect of Remove feeding (Air feeding) from flat-edge Bowtie nanoantenna

When removed the feeding of Bowtie nanoantenna with an (aluminum) material, which shown in Figure (2-8), The S-parameter, resonance frequency, and directivity were changed as seen in Figure (3-21), And Figure (3-22),

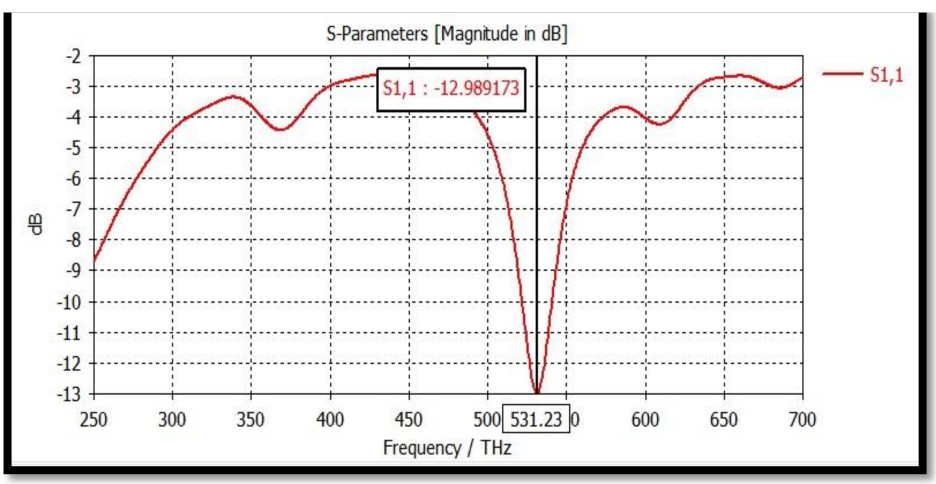

Figure 3.21: S-parameter and resonance frequency of flat-edge Bowtie nanoantenna in fig (2.8) when removing the feeding (Air feeding)

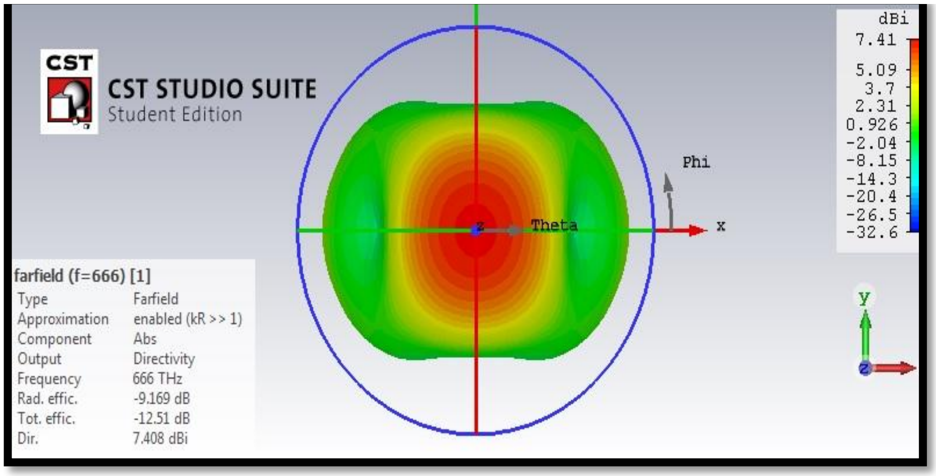

Figure 3.22: : The 3-d radiation pattern of flat-edge Bowtie nanoantenna in fig (2.8) when removing the feeding (Air feeding)

From Figure (3-21) and Figure (3-22), the S-parameter is found to be (-12.9 dB) at the resonance frequency of (531 THz), and the directivity is(7.41) at an incident frequency of(666 THz).

3.13 Effect of using a dielectric feeding for flat-edge Bowtie nanoantenna

In a Bowtie nanoantenna with an (Aluminum) material, shown in Figure (2-9), a dielectric feeding is used with the gab distance of (10 nm). The S-parameter, resonance frequency, and directivity are shown in Figure (3-23) and Figure (3-24),

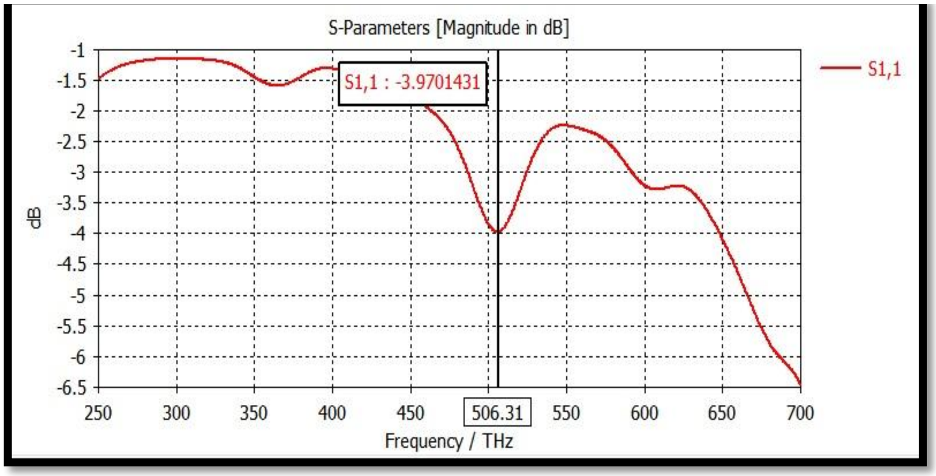

Figure 3.23: The : S-parameter and resonance frequency of flat-edge Bowtie nanoantenna in fig (2.9) when using a dielectric feeding

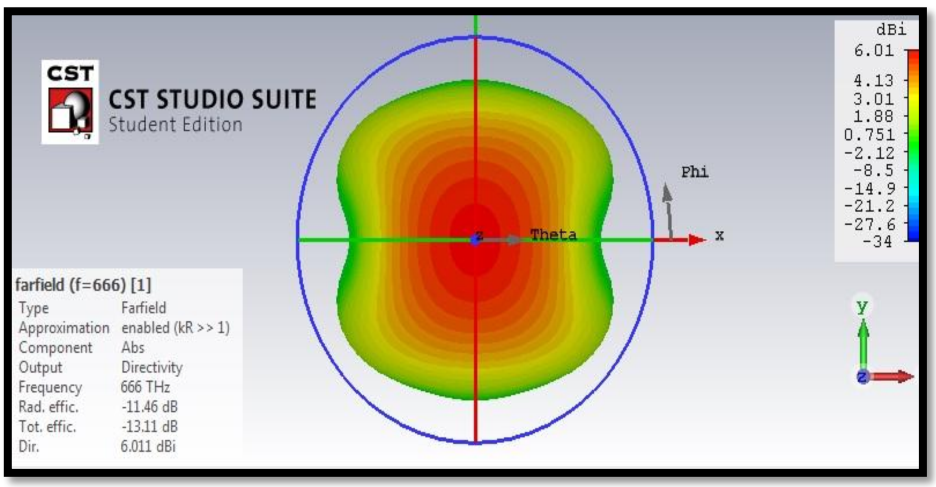

Figure 3.24: The 3-d radiation pattern of flat-edge Bowtie nanoantenna in fig (2.9) using a dielectric feeding

From Figure (3-23) and Figure (3-24), the S-parameter is (-3.9 dB) at a resonance frequency of (506.3 THz). and the directivity is (6.01) at an incident frequency of(666 THz).

3.14 Effect of removing the reflector from the flat-edge Bowtie nanoantenna

The effect of removing the reflector from the flat-edge Bowtie nanoantenna of Figure (2-10), is shown in Figures. (3-25), (3-26), and (3-27), with s-parameter of (-3.206 dB), and the directivity of (4.66) at resonance frequency (542 THz).

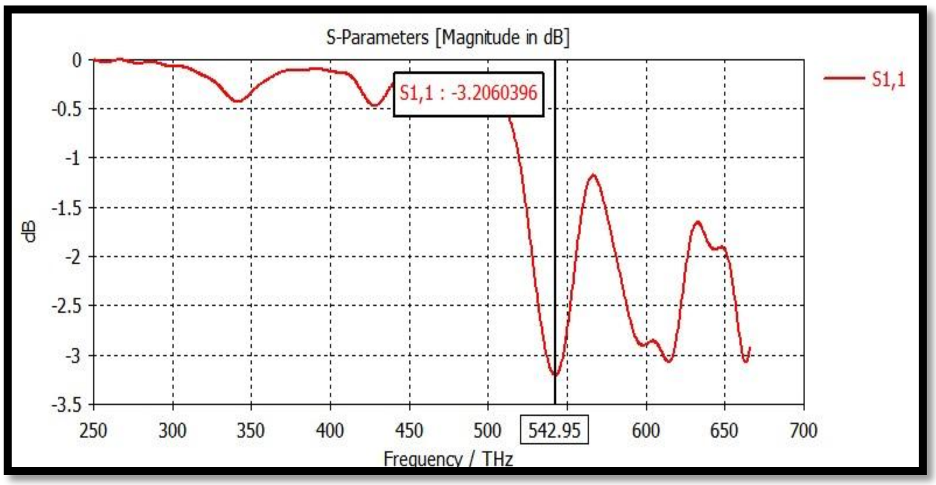

Figure 3.25: The result of S-parameter vs frequency of flat-edge Bowtie nanoantenna in fig (2.10) when removing the reflector

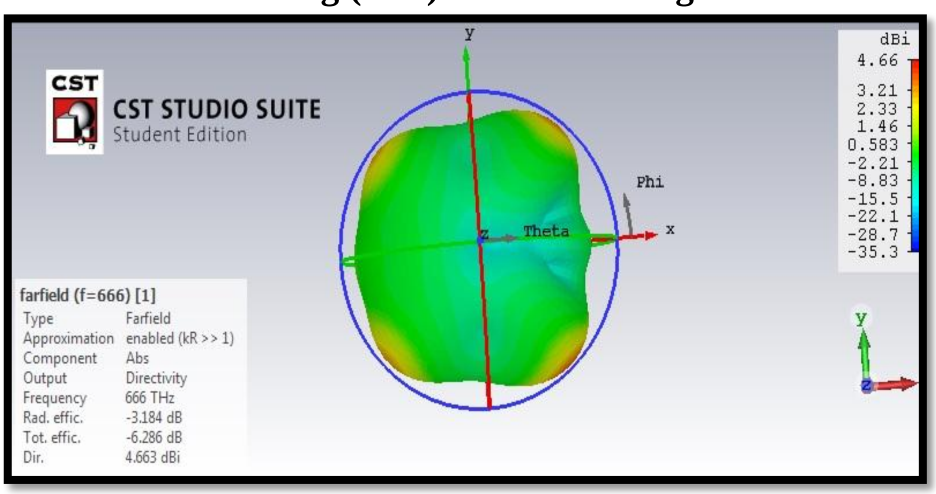

Figure 3.26: The 3-d radiation pattern of flat-edge Bowtie nanoantenna in fig (2.10) when removing the reflector

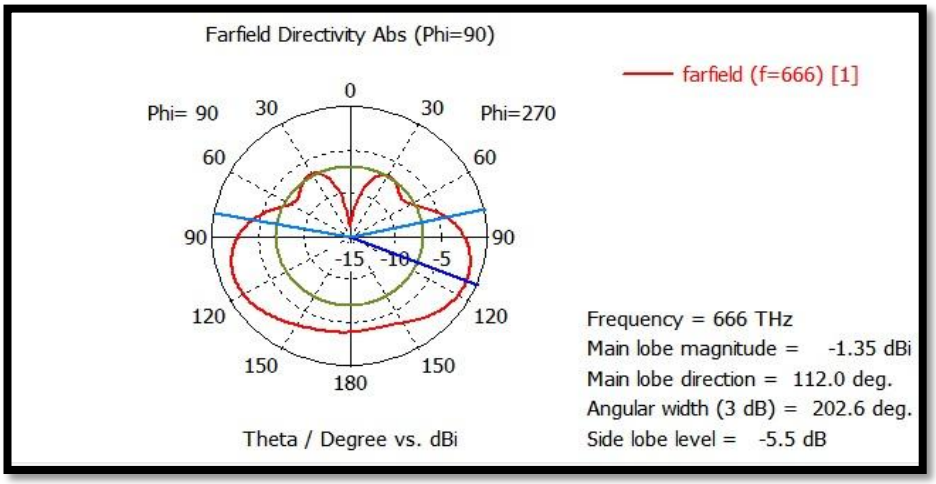

Figure 3.27: The polar plot of flat-edge Bowtie nanoantenna in fig (2.10) when removing the reflector

3.15 Conclusion

In this study, we have demonstrated the geometric and material effects which influence the performance of Bow-tie nanoantenna in the far-field region. We conclude that

- It was found that the optimum length for Bowtie nanoantenna is (130 nm) ,the width is (140 nm), the thickness is (20 nm), and , the gap distance of Bowtie nanoantenna (5 nm) with the gold material. The S-parameter is (-30 dB) and the resonance frequency is (377.3THz) .
- The highest near field was when the gap distance of bowtie nanoantenna was (30 nm) because of the resonance frequency was (310.23 THz) at that gap distance.
- Removing the feeding of flat edge Bowtie nanoantenna with an (aluminum) material, leads to an increase in the (s-parameter) to (-12.98 dB).
- The highest (S-parameter) was when we used the Aluminum material for Bowtie nanoantenna .
- When using feeding with a silver material, the s-parameter is the best (-9.567dB) and resonance frequency (301.73 THz).
- The highest directivity was when we used (Air feeding) for flat edge bowtie nanoantenna it was (7.14).
- All parameters of Bowtie optical nanoantenna are better than that of the flat-edge Bowtie nanoantenna.
- Feeding type and the Feeding shape of the nanoantenna do affect the resonance frequency and so it’s useful for matching conditions.

3.16 Future work

In our study, a practical study on the nanoantenna consisting of aluminum material on the SI substrate is presented, focusing on their favorite optical properties for the application of energy harvesting from infrared and THZ frequency region. There is some limitation in the presented design which requires improvement and further extension.

- The source utilized in the presented research is the single type plane wave excitation. Another type of light sources can be applied to illuminate nanoantenna
- This work is limited to simple geometrical structures such as, length of a nanoantenna, the width of the feeding, thickness of the substrate, and the gap between the antenna which are investigated in detail.Other dimensions can be investigated in the same way.

REFERENCES

[1] Novotny, L. and Hecht, B., 2012. *Principles of nano-optics*. Cambridge university press.

[2] Alu, A. and Engheta, N., 2013. Theory, modeling and features of optical nanoantennas. *IEEE Transactions on Antennas and Propagation*, *61*(4), pp.1508-1517.

[3] Scholder, O., 2014. *Fabrication, simulation and characterization of tunable plasmonic nano antennas* (Doctoral dissertation, ETH Zurich).

[4] Kılınç, M.C., 2010. *Resonant optical nanoantennas and applications* (Doctoral dissertation, bilkent university).

[5] Bharadwaj, P., Deutsch, B. and Novotny, L., 2009. Optical antennas. *Advances in Optics and Photonics*, *1*(3), pp.438-483.

[6] Alda, J., Rico-García, J.M., López-Alonso, J.M. and Boreman, G., 2005. Optical antennas for nano-photonic applications. *Nanotechnology*, *16*(5), p.S230.

[7] Ross, B.M. and Lee, L.P., 2009. Comparison of near-and far-field measures for plasmon resonance of metallic nanoparticles. *Optics letters*, *34*(7), pp.896-898.

[8] Novotny, L., 2007. Effective wavelength scaling for optical antennas. *Physical Review Letters*, *98*(26), p.266802.

[9] Chatterjee, R., 1996. *Antenna theory and practice*. New Age International.

[10] Willis, J.R., 2011. Effective constitutive relations for waves in composites and metamaterials. *Proceedings of the Royal Society A: Mathematical, Physical and Engineering Sciences*, *467*(2131), pp.1865-1879.

[11] Carletti, L., Locatelli, A., Neshev, D. and De Angelis, C., 2016. Shaping the radiation pattern of second-harmonic generation from AlGaAs dielectric nanoantennas. *ACS Photonics*, *3*(8), pp.1500-1507.

[12] Huang, J., Hao, Q., She, J. and Feng, Z., 2005, December. A six-port coupler with high directivity for VSWR measurement. In *2005 Asia-Pacific Microwave Conference Proceedings* (Vol. 4, pp. 4-pp). IEEE.

[13] Kumar, A., Hsu, K.H., Chaturvedi, P., Ma, H., Xu, J. and Fang, N.X., 2008, August. Fabrication and optical characterization of Bowtie antennas. In *2008 8th IEEE Conference on Nanotechnology* (pp. 98-99). IEEE.

[14] Yang, W., Chou Chau, Y.F. and Jheng, S.C., 2013. Analysis of transmittance properties of surface plasmon modes on periodic solid/outline Bowtie nanoantenna arrays. *Physics of Plasmas*, *20*(6), p.064503.

[15] Kumar, N. and Saini, G., 2013. A novel low profile planar inverted-f antenna (pifa) for mobile handsets. *International Journal of Scientific and Research Publications*, *3*(3), pp.3-6.

[16] Fung, C.W., 2011. Basic antenna theory and application.

[17] Knight, M.W., Liu, L., Wang, Y., Brown, L., Mukherjee, S., King, N.S., Everitt, H.O., Nordlander, P. and Halas, N.J., 2012. Aluminum plasmonic nanoantennas. *Nano letters*, *12*(11), pp.6000-6004.

[18] Ozbay, E., 2006. Plasmonics: merging photonics and electronics at nanoscale dimensions. *science*, *311*(5758), pp.189-193.

[19] Alduino, A. and Paniccia, M., 2007. Wiring electronics with light. *Nature Photonics*, *1*(3), pp.153-155.

[20] Heiblum, M., Wang, S., Whinnery, J. and Gustafson, T., 1978. Characteristics of integrated MOM junctions at dc and at optical frequencies. *IEEE Journal of Quantum Electronics*, *14*(3), pp.159-169.

[21] Bean, J.A., 2008. *Thermal infrared detection using antenna-coupled metal-oxide-metal diodes* (Doctoral dissertation).

[22] Shegai, T., Chen, S., Miljković, V.D., Zengin, G., Johansson, P. and Käll, M., 2011. A bimetallic nanoantenna for directional colour routing. *Nature communications*, *2*(1), pp.1-6.

[23] Schuller, J.A., Taubner, T. and Brongersma, M.L., 2009. Optical antenna thermal emitters. *Nature Photonics*, *3*(11), p.658.

[24] Anker, J.N., Hall, W.P., Lyandres, O., Shah, N.C., Zhao, J. and Van Duyne, R.P., 2010. Biosensing with plasmonic nanosensors. In *Nanoscience and Technology: A Collection of Reviews from Nature Journals* (pp. 308-319).

[25] Kumar, S. and Tanwar, S., 2016. Nanoantenna–A Review on Present and Future Perspective. *International Journal of Science Engineering & Technology*, *4*, pp.240-247.

[26] Reddy, T.S., Vyas, B.S., Avinash, T. and Ravi, T., Comparision Of Different Parameters On Cpw Fed Bowtie Antenna.

[27] Darzynkiewicz, Z., Holden, E., Orfao, A., Telford, W. and Wlodkowic, D. eds., 2011. *Recent advances in cytometry, Part A: Instrumentation, methods*. Academic Press.

[28] Adato, R., Yanik, A.A., Amsden, J.J., Kaplan, D.L., Omenetto, F.G., Hong, M.K., Erramilli, S. and Altug, H., 2009. Ultra-sensitive vibrational spectroscopy of protein monolayers with plasmonic nanoantenna arrays. *Proceedings of the National Academy of Sciences*, *106*(46), pp.19227-19232.

[29] Chen, T., Pourmand, M., Feizpour, A., Cushman, B. and Reinhard, B.M., 2013. Tailoring plasmon coupling in self-assembled one-dimensional Au nanoparticle chains through simultaneous control of size and gap separation. *The journal of physical chemistry letters*, *4*(13), pp.2147-2152.

[30] Fan, J.A., Wu, C., Bao, K., Bao, J., Bardhan, R., Halas, N.J., Manoharan, V.N., Nordlander, P., Shvets, G. and Capasso, F., 2010. Self-assembled plasmonic nanoparticle clusters. *science*, *328*(5982), pp.1135-1138.

[31] Hurtado-Aviles, E.A.; Torres, J.A.; Trejo-Valdez, M.; Urriolagoitia-Sosa, G.; Villalpando, I.; Torres-Torres, C. (28 October 2017). "Acousto-Plasmonic Sensing Assisted by Nonlinear Optical Interactions in Bimetallic Au-Pt Nanoparticles". Micromachines

[32] Chuntonov, L. and Haran, G., 2011. Effect of symmetry breaking on the mode structure of trimeric plasmonic molecules. *The Journal of Physical Chemistry C*, *115*(40), pp.19488-19495.

[33] Eustis, S. and El-Sayed, M.A., 2006. Why gold nanoparticles are more precious than pretty gold: noble metal surface plasmon resonance and its enhancement of the radiative and nonradiative properties of nanocrystals of different shapes. *Chemical society reviews*, *35*(3), pp.209-217.

[34] Zhang, J., Zhang, L. and Xu, W., 2012. Surface plasmon polaritons: physics and applications. *Journal of Physics D: Applied Physics*, *45*(11), p.113001.

[35] Manley, P., Burger, S., Schmidt, F. and Schmid, M., 2015. Design principles for plasmonic nanoparticle devices. In *Progress in Nonlinear Nano-optics* (pp. 223-247). Springer, Cham

[36] Perrotton, C., Javahiraly, N., Slaman, M., Dam, B. and Meyrueis, P., 2011. Fiber optic surface plasmon resonance sensor based on wavelength modulation for hydrogen sensing. *Optics express*, *19*(106), pp.A1175-A1183.

[37] Unser, S., Bruzas, I., He, J. and Sagle, L., 2015. Localized surface plasmon resonance biosensing: current challenges and approaches. *Sensors*, *15*(7), pp.15684-15716.

[38] Zayats, A.V. and Smolyaninov, I.I., 2003. Near-field photonics: surface plasmon polaritons and localized surface plasmons. *Journal of Optics A: Pure and Applied Optics*, *5*(4), p.S16.

[39] Chen, T., Pourmand, M., Feizpour, A., Cushman, B. and Reinhard, B.M., 2013. Tailoring plasmon coupling in self-assembled one-dimensional Au nanoparticle chains through simultaneous control of size and gap separation. *The journal of physical chemistry letters*, *4*(13), pp.2147-2152.

[40] Fernandez Garcia, R., 2013. Simulation and characterization of optical nanoantennas for field enhancement and waveguide coupling.

[41] Perkovac, M., 2012, May. Maxwell's equations for nanotechnology. In *2012 Proceedings of the 35th International Convention MIPRO* (pp. 429-436). IEEE.

[42] Kumar, A., Hsu, K.H., Chaturvedi, P., Ma, H., Xu, J. and Fang, N.X., 2008, August. Fabrication and optical characterization of Bowtie antennas. In *2008 8th IEEE Conference on Nanotechnology* (pp. 98-99). IEEE.

[43] Chen, W.Y. and Lin, C.H., 2010. Estimation of Electric Fields at Bow-tie Antenna Gaps.

[44] Yu-Ming, W., Le-Wei, L. and Bo, L., 2010, April. Geometric effects in designing bow-tie nanoantenna for optical resonance investigation. In *2010 Asia-Pacific International Symposium on Electromagnetic Compatibility* (pp. 1108-1111). IEEE.

[45] Thamae, L.Z. and Wu, Z., 2010. Broadband Bowtie dielectric resonator antenna. *IEEE Transactions on antennas and Propagation*, *58*(11), pp.3707-3710.

[46] Haque, A., Reza, A.W. and Kumar, N., 2015. A novel design of circular edge bow-tie nano antenna for energy harvesting. *Frequenz*, *69*(11-12), pp.491-499.

[47] Murad, F.A., Ali, F.M. and Hassan, A.A., 2016. Study the Effect of Change the Antenna Length on the Performance of Optical Nano-Antenna Using Plasmonic Surfaces. *journal of kerbala university*, *14*(2), pp.124-139.

[48] Pacheco-Peña, V., Beruete, M., Fernández-Domínguez, A.I., Luo, Y. and Navarro-Cía, M., 2017, July. Understanding Bowtie nanoantennas excited by a localized emitter. In *2017 IEEE International Symposium on Antennas and Propagation & USNC/URSI National Radio Science Meeting* (pp. 693-694). IEEE.

[49] Lee, T.S., Goyal, P., Li, C. and Zhao, K., 2018. Computational fluid dynamics to evaluate the effectiveness of inferior turbinate reduction techniques to improve nasal airflow. *JAMA facial plastic surgery*, *20*(4), pp.263-270.

[50] Jakšić, Z., Obradov, M., Vuković, S. and Belić, M., 2014. Plasmonic enhancement of light trapping in photodetectors. *Facta Universitatis, Series: Electronics and Energetics*, *27*(2), pp.183-203.

[51] Semiconductor, V., 2002. The general properties of si, ge, sige, sio2 and si3n4. *vol*, *10*, p.2012.

[52] Khaleque, A., Mironov, E.G., Osório, J.H., Li, Z., Cordeiro, C.M., Liu, L., Franco, M.A., Liow, J.L. and Hattori, H.T., 2017. Integration of bow-tie plasmonic nano-antennas on tapered fibers. *Optics express*, *25*(8), pp.8986-8996.

[53] Fromm, D.P., Sundaramurthy, A., Schuck, P.J., Kino, G. and Moerner, W.E., 2004. Gap-dependent optical coupling of single "Bowtie" nanoantennas resonant in the visible. *Nano letters*, *4*(5), pp.957-961.

[54] Laible, F., Gollmer, D.A., Dickreuter, S., Kern, D.P. and Fleischer, M., 2018. Continuous reversible tuning of the gap size and plasmonic coupling of bow tie nanoantennas on flexible substrates. *Nanoscale*, *10*(31), pp.14915-14922.

[55] Briones, E., Ruiz-Cruz, R., Briones, J., Gonzalez, N., Simon, J., Arreola, M. and Alvarez-Alvarez, G., 2018. Particle swarm optimization of nanoantenna-based infrared detectors. *Optics express*, *26*(22), pp.28484-28496.

[56] Davis, C.C., 1996. *Lasers and electro-optics: fundamentals and engineering*. Cambridge university press.

[57] Zhao, J.Y., Zhang, Z.Y., Liu, N.W., Fu, G. and Gong, S.X., 2014. Wideband unidirectional Bowtie antenna with pattern improvement. *Progress In Electromagnetics Research*, *44*, pp.119-124.

[58] Yang, J., Kong, F., Li, K. and Zhao, J., 2014. Optimizing the Bowtie nano-antenna for enhanced Purcell factor and electric field. *Progress In Electromagnetics Research*, *44*, pp.93-99.

[59] Choma, J., 2006. Scattering parameters: Concept, theory, and applications. *Univ. Southern California, Los Angeles, CA, USA, Tech. Rep. EE*, *541*(2).

[60] Balanis, C.A., 2016. *Antenna theory: analysis and design*. John wiley & sons.

[61] Krasnok, A.E., Maksymov, I.S., Denisyuk, A.I., Belov, P.A., Miroshnichenko, A.E., Simovski, C.R. and Kivshar, Y.S., 2013. Optical nanoantennas. *Physics-Uspekhi*, *56*(6), p.539.

List of publications(journal papers)

1- **Ghufran.A.Alkader, Jawad.A.Hassan" Design and study the performance of optical nanoantenna ", Alqadisiyah Journal for Engineering Sciences.**

(Published)

2- **Ghufran.A.Alkader, Jawad.A.Hassan “Enhancement of electric field of Bowtie nanoantenna”, Muthanna Journal of Engineering and Technology**

(Published)

الخـلاصـــة

تم استخدام هوائي النانو في العديد من التطبيقات في مجال الاتصالات لنقل البيانات لاسلكيًا بمعدلات عالية جدًا ، والطب ، والكيمياء وتقنيات (التيراهيرتز) , وتطبيقات النانوفوتونية ، في هذه الدراسة ، يهدف البحث إلى دراسة الأداء وتردد الرنين ، كفاءة الانعكاس ,والاتجاهية , لهوائي (الباوتاي) بأبعاد مختلفة مثل (مسافة الفجوة ، السماكة ، والزاوية) لهوائي النانو (باوتاي) وبمواد مختلفة مثل (الذهب, والنيكل, والفضة,والالمنيوم تمت دراسة برنامج نانو انتينا بووتي باستخدام برنامج تكنولوجيا المحاكاة الحاسوبية (cst) باستخدام تقنية التكامل المحدود (FIT).

لتصميم نوعين من نانو انتينا باوتاي (نانو انتينا باوتاي بحافة مدببة و نانو انتينا باوتاي بحافة مسطحة) يتم وضعه على مادة عازلة للحصول على بلازما هوائي النانو ، وشرح كيفية تأثر استجابة هوائي نانو باوتاي بتغيير أبعاده والمواد المستخدمة في تصميمه.

وقد وجد ان الطول الأمثل للهوائي كان (130 نانومتر) ، وعرض الهوائي (140 نانومتر) ، وسمك الهوائي (20 نانومتر) ، والمادة المستخدمة في تصميم الهوائي هي الذهب ، ومسافة الفجوة بين جزأين الهوائي (5 نانومتر) مع مادة الذهب ، حيث كانت كفاءة الانعكاس (33− ديسيبل). وكان تردد الرنين (377.3 تيراهيرتز).

وكان المجال الكهربائي القريب الأعلى عندما كانت مسافة الفراغ بين جزأين الهوائي (30 نانومتر) وذلك بسبب انه تردد موجة الرنين (310.23 تيراهيرتز) عند هذه المسافة.

ونستنتج من ذلك إلى أن مسح التغذية من وسط هوائي النانو ذو الحافة المسطحة يؤدي الى زيادة كفاءة الانعكاس الى (12.98 dB−).

جمبع نتائج هوائي النانو انتنا ذو الحافة المدببة هي افضل من هوائي النانو ذو الحافة المسطحة و يمكن استخدام هذا هوائي النانو (باوتاي) في العديد من التطبيقات كما هو الحال في مجال الاتصال لأنه يمكن أن يعمل على ترددات متعددة.ومجال الطب والبيولوجي .

وزارة التعليم العالي والبحث العلمي
جامعـــــة بـغداد
معهد الليزر للدراسات العليـــا

المبادئ الاساسية لهوائي النانو البصري (باوتاي)

رسالة مقدمة الى

معهد الليزر للدرسات العليا /جامعة بغداد /لاستكمال متطلبات نيل شهادة ماجستير في الليزر /الهندسة الالكترونية والاتصالات

من قبل

غفران عبد القادر حسن

بكالوريوس هندسة الليزر والالكترونيات البصرية

2008

باشراف

م.د جواد عبد الكاظم حسن

1441هـ 2020 م